The clinical implication and molecular mechanism of preferential IL-4 production by modified glycolipid-stimulated NKT cells

Shinji Oki, Asako Chiba, Takashi Yamamura, and Sachiko Miyake

Department of Immunology, National Institute of Neuroscience, National Center for Neuroscience and Psychiatry, Tokyo, Japan.

OCH, a sphingosine-truncated analog of α-galactosylceramide (αGC), is a potential therapeutic reagent for a variety of Th1-mediated autoimmune diseases through its selective induction of Th2 cytokines from natural killer T (NKT) cells. We demonstrate here that the NKT cell production of IFN-γ is more susceptible to the sphingosine length of glycolipid ligand than that of IL-4 and that the length of the sphingosine chain determines the duration of NKT cell stimulation by CD1d-associated glycolipids. Furthermore, IFN-γ production by NKT cells requires longer T cell receptor stimulation than is required for IL-4 production by NKT cells stimulated either with immobilized mAb to CD3 or with immobilized "αGC-loaded" CD1d molecules. Interestingly, transcription of *IFN-γ* but not that of *IL-4* was sensitive to cycloheximide treatment, indicating the intrinsic involvement of de novo protein synthesis for IFN-γ production by NKT cells. Finally, we determined *c-Rel* was preferentially transcribed in αGC-stimulated but not in OCH-stimulated NKT cells and was essential for IFN-γ production by activated NKT cells. Given the dominant immune regulation by the remarkable cytokine production of ligand-stimulated NKT cells in vivo, in comparison with that of (antigen-specific) T cells or NK cells, the current study confirms OCH as a likely therapeutic reagent for use against Th1-mediated autoimmune diseases and provides a novel clue for the design of drugs targeting NKT cells.

Introduction

Natural killer T (NKT) cells are a unique subset of T lymphocytes that coexpress the α/β T cell receptor (TCR) along with markers of the NK lineage such as NK1.1, CD122, and various Ly49 molecules. Most NKT cells express an invariant TCRα chain composed of Vα14-Jα281 segments in mice and Vα24-JαQ segments in humans associated with a restricted set of Vβ genes (1, 2). Unlike conventional T cells, which recognize peptides presented by MHC molecules, NKT cells recognize glycolipid antigens such as α-galactosylceramide (αGC) in the context of a nonpolymorphic MHC class I–like molecule, CD1d (3–5). After being stimulated by a ligand, NKT cells rapidly affect the functions of neighboring cell populations such as T cells, NK cells, B cells, and dendritic cells (6, 7). The various functions of NKT cells are mediated mainly by a rapid release of large amounts of cytokines, including IL-4 and IFN-γ. Whereas IFN-γ provides help for the Th1 responses required for defending against various pathogens and tumors, IL-4 controls the initiation of Th2 responses and has been shown to inhibit Th1-mediated autoimmune responses involved in experimental autoimmune encephalomyelitis (EAE), collagen-induced arthritis (CIA), and type 1 diabetes in NOD mice.

Given the exceptional ability of NKT cells to secrete regulatory cytokines in comparison with that of T cells or NK cells after primary stimulation, we have explored the possibility that

ligand stimulation of NKT cells may lead to the suppression of Th1-mediated autoimmune diseases. We have previously demonstrated that OCH, a sphingosine-truncated analog of αGC, preferentially induces Th2 cytokines from NKT cells and that administration of OCH suppresses EAE and CIA by inducing a Th2 bias in autoantigen-reactive T cells (8, 9). However, the molecular mechanism accounting for the unique property of OCH to selectively induce IL-4 has not been clarified yet.

In this study, we used various stimuli, including the prototypic ligand αGC and its derivatives such as OCH, to investigate the molecular basis of the differential production of IL-4 and IFN-γ by NKT cells. We found that OCH, due to its truncated lipid chain, was less stable in binding the CD1d molecule than was αGC and exerted short-lived stimulation on NKT cells. IFN-γ production by NKT cells required longer TCR stimulation than was required for IL-4 production and de novo protein synthesis. *c-Rel* was preferentially transcribed in αGC-stimulated, but not in OCH-stimulated NKT cells and was shown to regulate IFN-γ production by NKT cells. Taken together, these results indicate that sustained TCR stimulation and concomitant c-Rel expression by αGC leads to the production of IFN-γ, whereas short-term activation and marginal *c-Rel* transcription by OCH results in preferential production of IL-4 by NKT cells.

Methods

Mice. C57BL/6 (B6) mice were purchased from CLEA Laboratory Animal Corp. (Tokyo, Japan). MHC class II–deficient I-Aᵇ⁻/⁻ mice were purchased from Taconic (Germantown, New York, USA). All animals were kept under specific pathogen-free conditions and were used at 7–10 weeks of age. Animal care and use were in accordance with institutional guidelines.

Cell lines, antibodies, plasmids, and reagents. The NKT cell hybridoma (N38.2C12) (10) was a generous gift from K. Hayakawa (Fox Chase Cancer Center, Philadelphia, Pennsylvania, USA) and NS0-derived

plasmacytoma cell lines expressing the Kb tail mutant of CD1d (11) were kindly provided by S. Joyce (Vanderbilt University, Nashville, Tennessee, USA). Cells were maintained in RPMI 1640 medium supplemented with 10% FCS, 2 mM L-glutamine, 100 U/ml penicillin/ streptomycin, 2 mM sodium pyruvate, and 50 μM β-mercaptoethanol (complete medium). Phycoerythrin (PE)-labeled mAb to NK1.1 (PK136), peridinine chlorophyll protein/cyanine 5.5 –labeled mAb to CD3 (2C11), and recombinant soluble dimeric human CD1d:Ig fusion protein (DimerX I) were from BD PharMingen (San Diego, California, USA). For some experiments mAb's to NK1.1 (PK136) and CD3 (2C11) were conjugated with FITC. Polyclonal antibody to asialo GM₁ was purchased from WAKO Chemicals (Osaka, Japan). The pRc/CMV-c-Rel expression plasmid (12) was a generous gift from Grundström (Umeå University, Umeå, Sweden). The open reading frame of c-Rel cDNA was amplified by PCR and cloned into the retroviral pMIG(W) vector. The forward primer containing the *Xho*I recognition site was 5'-GACTCTCGAGATGGCCTCGAGTG-GATATAA-3' and the reverse primers used for wild-type c-Rel or the dominant negative mutant c-RelΔTA containing *Eco*RI recognition sites were 5'-GACTGAATTCTTATATTTTAAAAAAACCATATGT-GAAGG-3' and 5'-GACTGAATTCTTAACTCGAGATGGACCCG-CATG-3', respectively. The retroviral vector (pMIG) and packaging vector (pCL-Eco) were kindly provided by L. Van Parijs (Massachusetts Institute of Technology, Cambridge, Massachusetts, USA). Cyclosporin A (CsA) and cycloheximide (CHX) were from Sigma-Aldrich (St. Louis, Missouri, USA). All glycolipids were prepared as described in the Supplemental Methods (supplemental material available at http://www.jci.org/cgi/content/full/113/11/1631/ DC1). The glycolipids were solubilized in DMSO (100 μg/ml) and were stored at -20°C until use.

Kinetic analysis of glycolipid stability on CD1d molecules. The kinetic analysis of glycolipid stability on CD1d molecules was performed as described previously with slight modifications (13). In brief, the NKT hybridoma was preincubated with 4 μM Fura red and 2 μM Fluo-4 (Molecular Probes, Eugene, Oregon, USA) at room temperature for 45 minutes, washed with RPMI 1640 medium containing 2% FCS (assay media), and resuspended in assay media. For determination of the optimal time for glycolipid loading onto CD1d⁺ APCs, kinetic analysis was conducted using either αGC or OCH. According to the data obtained in Figure 2C, CD1d⁺ APCs were pulsed with glycolipids (100 ng/ml) for 30 minutes. Then, cells were washed and resuspended in assay media. Glycolipid-pulsed APCs were harvested every 15 minutes after resuspension, mixed with NKT cells, and subjected to centrifugation in a table-top centrifuge (2,000 g) for 60 seconds. Cells were then resuspended briefly and analyzed for calcium influx into NKT hybridoma cells by flow cytometry (EPICS XL; Beckman Coulter, Tokyo, Japan). Activation was expressed as the percentage of Fura-red– and Fluo-4–stained cells in a high-FL1, low-FL4 gate.

In vivo glycolipid treatment and microarray analysis. Mice were injected intraperitoneally with 0.2 ml PBS containing 0.1 mg anti-asialo GM₁ Ab. Forty hours after injection, mice were injected intraperitoneally with αGC, OCH (100 μg/kg), or control vehicle in 0.2 ml PBS. After the indicated time point, liver mononuclear cells or spleen cells were harvested and NKT cells were purified with the AUTOMACS cell purification system using FITC-conjugated mAb to NK1.1 (PK136) and anti-FITC microbeads (Miltenyi Biotech GmbH, Bergisch Gladbach, Germany). The purity of NKT cells in the untreated samples and in the samples treated for 1.5 hours was more than 90%. The purity of the liver-derived samples

and spleen-derived samples treated for 12 hours was more than 80% and 74%, respectively. Total RNA isolation with the RNeasy Mini Kit (Qiagen, Chatsworth, California, USA) and whole-microarray procedures using U74Av2 arrays (GeneChip System; Affymetrix, Santa Clara, California, USA) were done according to the manufacturers' instructions. From data image files, gene transcript levels were determined using algorithms in the Gene Chip Analysis Suit software (Affymetrix). Each probe was assigned a "call" of present (expressed) or absent (not expressed) using the Affymetrix decision matrix. Genes were considered to be differentially expressed when (a) expression changed at least threefold in the case of liver NKT-derived samples or twofold in the case of spleen NKT-derived samples compared with the expression in the negative control and (b) increased gene expression included at least one "present call."

In vitro stimulation. Liver mononuclear cells were isolated from B6 mice by Percoll density gradient centrifugation and were stained with PE-NK1.1 and FITC-CD3 mAb's. The CD3⁺NK1.1⁺ cells and CD3⁺NK1.1⁻ cells were sorted with an EPICS ALTRA Cell Sorting System (Beckman Coulter). The purity of the sorted cells was more than 95%. Sorted cells were suspended in RPMI 1640 medium supplemented with 50 μM 2-mercaptoethanol, 2 mM L-glutamine, 100 U/ml penicillin and streptomycin, and 10% FCS and were stimulated with immobilized mAb to CD3. Incorporation of [³H]thymidine (1 μCi/well) for the final 16 hours of the culture was analyzed with a β-1205 counter (Pharmacia, Uppsala, Sweden). We measured the content of cytokines in the culture supernatants by ELISA. For quantitative PCR analysis, we harvested the cells after stimulation with glycolipid to prepare total RNA. Glycolipid stimulation of spleen cells in vitro was done similarly except that 1% syngeneic mouse serum was used instead of FCS. In some experiments, plates were coated with DimerX I (1 μg in 50 μl PBS per well) for 16 hours. After plates were washed extensively with PBS, glycolipids (100-200 ng in 50 μl PBS per well) were added, followed by incubation for another 24 hours. Then, NKT cells were added and cytokine production was analyzed after 72 hours of incubation.

Real-time PCR to monitor gene expression. Real-time PCR was conducted using a Light Cycler-FastStart DNA Master SYBR Green I kit (Roche Diagnostics GmbH, Mannheim, Germany) according to the manufacturer's specifications using 4 mM MgCl₂ and 1 pM primers. Values for each gene were normalized to those of a housekeeping gene (*GAPDH*) before the "fold change" was calculated (using crossing point values) to adjust for variations between different samples. Primers used for the analysis of gene expression are described in Supplemental Methods.

ELISA. For evaluation of cytokine production by NKT cells, sorted liver CD3⁺NK1.1⁺ NKT cells were stimulated with immobilized mAb to CD3 in complete medium. The level of cytokine production in cell culture supernatants or in serum was determined by standard sandwich ELISA using purified and biotinylated mAb sets and standards from BD PharMingen. After the addition of a substrate, the reaction was evaluated using a Microplate reader (BioRad).

Retroviral infection of NKT cells. The 293T cells were maintained in DMEM supplemented with 10% FCS, 2 mM L-glutamine, 100 U/ml penicillin/streptomycin, 2 mM sodium pyruvate, and 50 μM β-mercaptoethanol. Liver mononuclear cells were purified and cultured in complete medium supplemented with IL-2 (200 U/ml) for 24-48 hours. Cells were infected with retrovirus prepared by cotransfection of pMIG retroviral vector and pCL-Eco packaging vector into 293T cells. Cells were cultured in complete medium containing IL-2 and IL-15 (50 ng/ml) continuously for 3 days, and
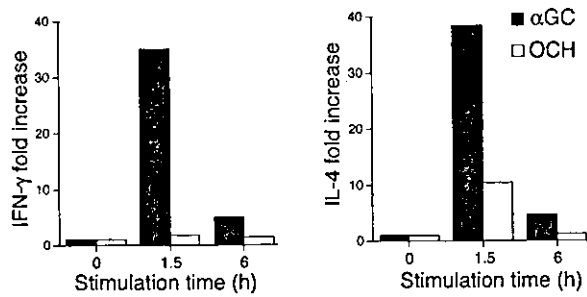
Figure 1

Transcriptional upregulation of cytokine genes by NKT cells stimulated with glycolipids in vivo. B6 mice were injected intraperitoneally with αGC or OCH (100 μg/kg), and liver NKT cells were isolated at the indicated time point. Total RNA was extracted and analyzed for cytokine mRNA by quantitative RT-PCR as described in Methods. Data are presented as "fold induction" of cytokine mRNA after glycolipid treatment. The amount of mRNA in NKT cells derived from untreated animals was defined as 1.

GFP-positive NKT cells were sorted and stimulated with immobilized mAb to CD3 for 48 hours. Culture supernatants were subjected to evaluation of cytokine production by ELISA.

Results

Preferential IL-4 production by OCH-stimulated NKT cells. The suppression of EAE by OCH was found to be associated with a Th2 bias of autoimmune T cells mediated by IL-4 produced by NKT cells (9). To confirm the primary involvement of NKT cells in the Th2 bias seen in the OCH treatment, we purified CD3⁺NK1.1⁺ NKT cells from B6 mice treated in vivo with αGC or OCH and measured the transcription of cytokine genes by quantitative RT-PCR. As shown in Figure 1, treatment with αGC greatly increased the expression of both IFN-γ and IL-4 at 1.5 hours after injection, whereas OCH induced a selective increase in IL-4 expression. When the IL-4/IFN-γ ratio was used for evaluating the Th1/Th2 balance, the NKT cells, isolated at 1.5 hours after injection of OCH were distinctly biased toward Th2 (Table 1). These results indicate that OCH is a selective inducer of rapid IL-4 production by NKT cells when administered in vivo.

Lipid chain length and cytokine production. Comparison of the structural difference between OCH and αGC (Figure 2A) raised the possibility that the lipid chain length of the glycolipid ligand may influence the cytokine profile of glycolipid-treated NKT cells. We compared αGC and OCH as well as newly synthesized analogs F-2/S-3 and F-2/S-7, which bear lipids of intermediate length (Figure 2A), for their ability to induce cytokine production by splenocytes. There was good correlation between the lipid tail length of each glycolipid and its ability to induce IFN-γ from the splenocytes, and a larger amount of IFN-γ was released into the supernatants after stimulation with the glycolipids with the longer sphingosine chain (Figure 2B, right). Regarding the ability to stimulate IL-4 production, the differences among OCH, F-2/S-3 and F-2/S-7 were less clear, as shown by IFN-γ induction. Similar results were obtained with liver mononuclear cells as responder cells (see Supplemental Figure 1). These results indicate that cytokine production by NKT cells, in particular IFN-γ production, is greatly influenced by lipid chain truncation of the glycolipid.

Differential half-life of NKT cell stimulation by CD1d-associated glycolipids. It is believed that the two lipid tails of the glycolipids (sphingosine base and fatty acyl chain) would be accommodated by the highly hydrophobic binding grooves of CD1d. To verify the hypothesis

that the functional properties of each glycolipid may be determined by the stability of its binding to CD1d molecules, we evaluated the half-life of these glycolipids on CD1d molecules by estimating calcium influx into NKT hybridoma cells as described previously (13). To exclude the possible involvement of endosomal/lysosomal sorting in this assay, we used APCs expressing a CD1d mutant (Kb tail) that lacks the endosomal/lysosomal targeting signal (11). The cells express both β2m and sCD1d1 fused to the transmembrane and cytosolic tail sequence of H-2Kᵇ at the carboxyl terminus and could bind to glycolipids such as αGC or OCH without their internalization and following endosomal/lysosomal sorting. Based on the kinetic analysis data for glycolipid loading efficiency shown in Figure 2C, we pulsed CD1d⁺ APCs with glycolipids for 30 minutes.

Figure 2D shows that OCH was rapidly released from the CD1d molecule. A 30% reduction in calcium influx was observed after 15 minutes of incubation and only 25% of the initial amount of glycolipid remained after 60 minutes of incubation. In contrast, αGC was not released from CD1d molecule in the first 15 minutes and more than 50% of the initial amount of glycolipid remained after 60 minutes of incubation. F-2/S-3 and F-2/S-7 showed intermediate levels of release from CD1d molecule. These results support the idea that a glycolipid with a shorter sphingosine chain has a shorter half-life for NKT cell stimulation because of less-stable association with the CD1d molecule.

Kinetic analysis of cytokine production by activated NKT cells. Previous in vivo studies demonstrated that injection of αGC into B6 mice can induce a rapid and transient elevation of the serum IL-4 level and a delayed and persistent rise in IFN-γ (9, 14), suggesting that there is an intrinsic difference in kinetics for the production of IL-4 and IFN-γ by NKT cells. To address this issue further, we sorted CD3⁺NK1.1⁺ NKT cells, and conventional CD3⁺NK1.1⁻ T cells as a control, from liver lymphocytes and stimulated the sorted cells with immobilized mAb to CD3 for various periods of time. The cells were then incubated at rest without further stimulation and culture supernatants were harvested at 72 hours after initiation of the TCR stimulation. We found that TCR stimulation of NKT cells for as little as 2 hours could induce detectable IL-4 in the supernatant (Figure 3A, center). The amount of IL-4 in the supernatant rapidly increased in proportion to the duration of TCR stimulation (Figure 3A, center). In contrast, production of IFN-γ by NKT cells required at least 3 hours of TCR stimulation and gradually increased corresponding to the duration of TCR stimulation (Figure 3A, right). Conventional T cells required longer TCR stimulation for efficient cytokine production. We repeatedly confirmed that IFN-γ production by NKT cells required initial stimulation that was 1-2 hours longer and showed a slower accumulation than that of IL-4 production in this experimen-

Table 1

Transcriptional upregulation of cytokine genes by NKT cells stimulated with glycolipids in vivo

Stimulus	Time	IFN-γ	IL-4	Ratio (IL-4/IFN-γ)
αGC	1.5 h	35.0	38.3	1.09
	6 h	5.0	4.6	0.92
OCH	1.5 h	1.8	10.3	5.58
	6 h	1.5	1.1	0.72

The relative amounts of transcripts of *IFN-γ* and *IL-4* obtained from the experiment shown in Figure 1 are presented as "fold induction" relative to that of NKT cell–derived samples from untreated animals.
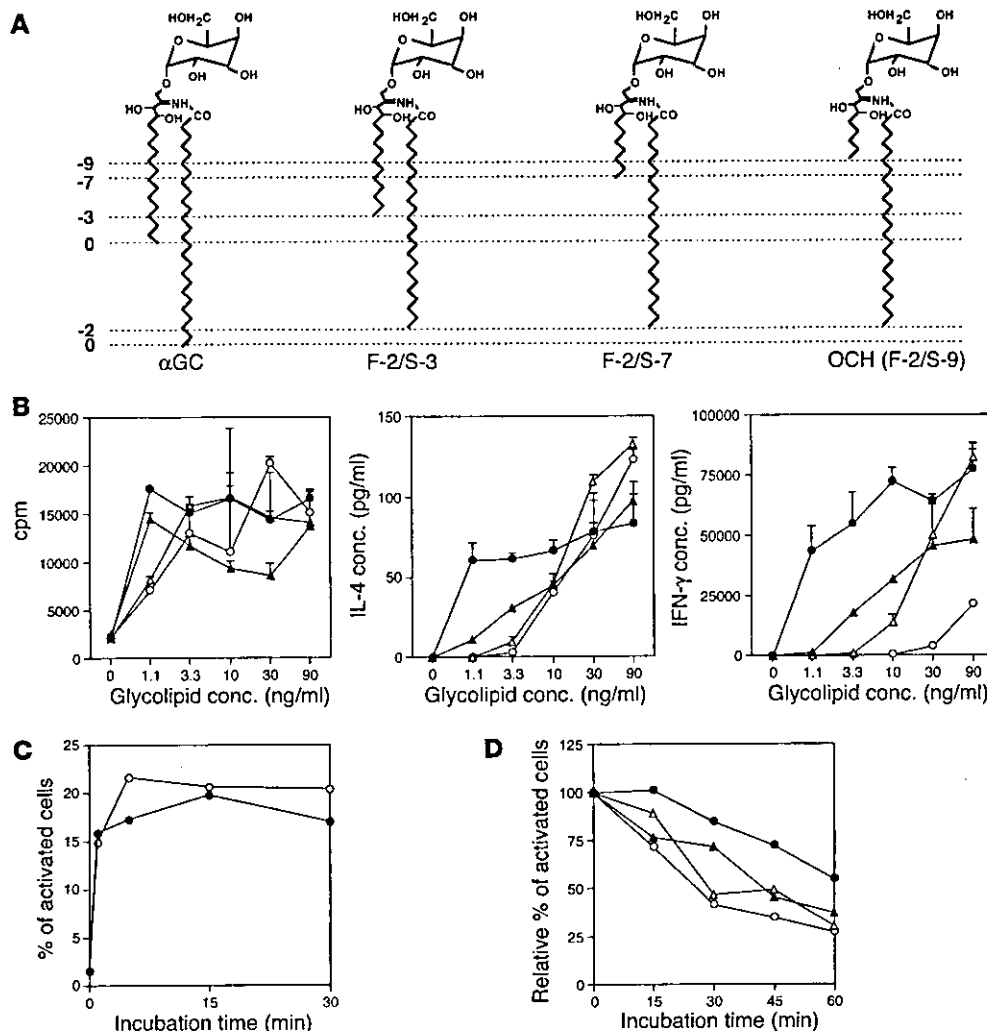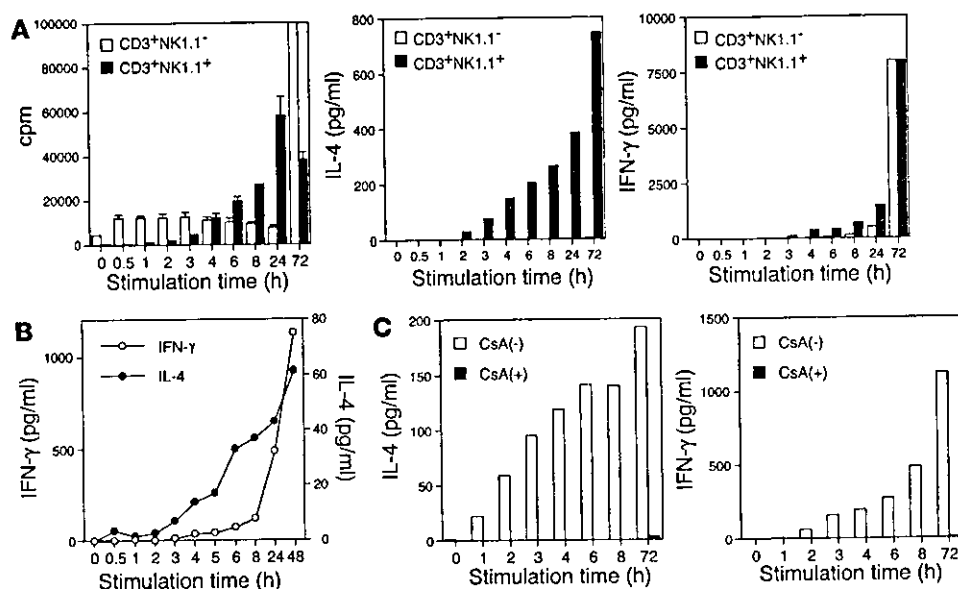
Figure 2
Differential properties of structurally distinct glycolipid derivatives. (**A**) Structures of αGC, OCH, and two other glycolipid ligands for NKT cells. F-2/S-3 has a truncation of two hydrocarbons in the fatty acyl chain (F) and of three hydrocarbons in the sphingosine chain (S) in comparison with αGC. OCH can be called F-2/S-9 accordingly. The numbers of truncated hydrocarbons in either lipid chain are shown along the left margin as negative integers. (**B**) Effect of αGC, OCH, and other glycolipids on proliferation and cytokine production of splenocytes. Splenocytes were stimulated with various concentrations (conc.) of αGC (filled circles), OCH (open circles), F-2/S-3 (filled triangles), or F-2/S-7 (open triangles) for 72 hours. Incorporation of [³H]thymidine (1 μCi/well) during the final 16 hours of the culture was assessed (left), and IL-4 (center) or IFN-γ (right) in the supernatants was measured by ELISA. (**C**) Kinetic analysis of the loading of αGC (filled circles) or OCH (open circles) onto CD1d⁺ APCs. See Methods for details. One experiment representative of two independent experiments with similar results is shown. (**D**) Calcium influx into NKT hybridoma cells after coculture with CD1d⁺ APCs pulsed with αGC, OCH, F-2/S-3, or F-2/S-7. Data are presented as the activity remaining when the respective activity of glycolipid-loaded APCs for activation of the NKT cell hybridoma at time 0 was defined as 100%. Data are representative of three experiments with similar results.

tal setting. A similar kinetic difference was also observed when we used spleen-derived NKT cells (data not shown). These results indicate that NKT cells could produce IL-4 after a shorter period of TCR stimulation than is required for IFN-γ production.

To exclude the possibility that a qualitatively different CD1d complex with either αGC or OCH may bind with altered affinity to the TCR, we stimulated NKT cells with plate-bound αGC-CD1d complexes instead of mAb to CD3 for the periods of time indicated in Figure 3B. Consistent with the previous results obtained with anti-CD3 stimulation, the level of IL-4 in the culture supernatant was increased after shorter periods of incubation. In contrast, IFN-γ was efficiently produced after longer incubation, showing

that the short pulse of NKT cells with plate-bound αGC-CD1d complexes could recapitulate the OCH phenotype. These results demonstrate that the timing of the CD1d-lipid interaction rather than the "shape" of the OCH-CD1d complex is the decisive factor in controlling polarization of cytokine production by NKT cells.

Differential transcriptional properties of cytokine genes. To clarify the molecular basis for different kinetics of cytokine production by activated NKT cells, we next examined the effects of CsA or CHX on the NKT cell responses. Without any inhibitors, IL-4 production was more rapid and had a higher rate than IFN-γ production (Figure 3C), confirming the kinetic difference required for induction of each cytokine shown in Figure 3A. Production of both IL-4

Figure 3
Kinetic analysis of NKT cell activation and cytokine production after glycolipid stimulation. (A) Differential production of IFN-γ and IL-4 by activated NKT cells. CD3⁺NK1.1⁺ NKT cells and conventional CD3⁺NK1.1⁻ T cells were purified from liver mononuclear cells by cell sorting. The sorted cells were stimulated with immobilized mAb to CD3 for the time indicated on the x axis and were then removed and recultured on a fresh culture plate without anti-CD3 stimulation for up to 72 hours from the start of the anti-CD3 stimulation. Incorporation of [³H]thymidine (1 μCi/well) during the final 16 hours of the culture was assessed (left), and culture supernatants were analyzed for the production of IL-4 (center) and IFN-γ (right) by ELISA. One experiment representative of three independent experiments with similar results is shown. (B) NKT cells purified from liver mononuclear cells were stimulated with plates coated with DimerX I loaded with αGC and were analyzed as shown in A. (C) NKT cells purified from liver mononuclear cells were stimulated as shown in A in the presence [CsA(+)] or absence [CsA(−)] of CsA (1 μg/ml). Culture supernatants were analyzed for the production of IL-4 and IFN-γ by ELISA.

and IFN-γ after TCR stimulation, however, was almost completely inhibited by pretreatment of NKT cells with CsA.

Similarly, CsA abolished the transcriptional activation of IL-4 and IFN-γ genes in activated NKT cells (Figure 4A), indicating that TCR signal–induced activation of nuclear factor of activated T cell (NF-AT) is indispensable for the production of both cytokines by NKT cells. Meanwhile, transcription of these cytokine genes showed different sensitivities to CHX treatment (Figure 4A). Although transcriptional activation of IL-4 was barely affected by CHX treatment, transcription of IFN-γ gene was almost completely blocked after treatment with CHX. These results indicate that transcriptional activation of IFN-γ, but not that of IL-4, requires de novo protein synthesis.

Next, we analyzed the sensitivities of other cytokine genes to CsA and CHX treatment (15–17). As shown in Figure 4B, transcriptional activation of all cytokine genes tested was completely blocked by pretreatment of NKT cells with CsA. Interestingly, transcription of the IL-2 gene and GM-CSF gene were blocked by CHX treatment. In contrast, transcriptional activation of TNF-α was resistant to CHX treatment. These results indicate that cytokines produced by NKT cells could be divided into two groups based on their dependence on de novo protein synthesis.

Selective c-Rel induction after stimulation with αGC. Although NKT cells secrete a large number of cytokines upon stimulation, the regulatory mechanisms for the expression of each cytokine are still poorly understood. The susceptibility of IFN-γ production to CHX indicates that some newly synthesized protein(s) would promote specific tran-

scription of the IFN-γ gene in NKT cells. To identify the protein responsible for αGC-induced transcription of the IFN-γ gene, we purified NKT cells from glycolipid-administered I-Aᵇβ-deficient mice, which have two- to threefold higher numbers of NKT cells in the liver and the spleen than do wild-type B6 mice (18), and assessed NKT cell–derived total RNA by microarray analysis. As shown in Table 2, a number of cytokines and chemokines were differentially expressed after in vivo treatment with either αGC or OCII. It is noteworthy, however, that significant induction of IFN-γ transcription was observed only in αGC-treated samples, not in OCH-treated samples. Overall, the data obtained correlated well with previous results showing that OCII is a selective inducer of IL-4 production from NKT cells (9). There was no transcriptional upregulation of cytokines genes such as the IFN-γ and IL-4 genes 12 hours after treatment with either glycolipid, indicating that NKT cells have undergone quiescence at this time point in the context of transcriptional upregulation of cytokine genes, although some genes are still upregulated.

Through analyzing the microarray data, we identified the protooncogene c-Rel, a member of the NF-κB family of transcription factors, as a candidate molecule that may play a role in the IFN-γ transcription. As shown in Figure 5A, c-Rel was inducibly expressed in NKT cells 1.5 hours after stimulation with αGC. In contrast, OCH treatment did not induce c-Rel transcription (Figure 5A). The transcription of other NF-κB family genes such as p65/RelA and RelB was not upregulated after treatment with αGC or OCH. Real-time PCR analysis also confirmed the selective induction of c-Rel after αGC stimulation (Figure 5B). CsA treatment inhibited c-Rel transcription, but CHX did not (Figure 5C), indicating that the inducible transcription of c-Rel is directly controlled by TCR signal–mediated activation of the NF-AT (19).

It is already known that c-Rel serves as a pivotal transcription factor for the Th1 response that would directly induce IFN-γ production in conventional T cells (20). However, very little is known about the function of this protooncogene in NKT cells during TCR-mediated activation. We therefore conducted time course analysis for transcriptional activation of c-Rel in parallel with IL-4 and IFN-γ. We stimulated NKT cells with immobilized mAb to CD3 for 30–100 minutes and then cultured them without further stimulation for a total of 120 minutes. As shown in Figure 5D, IFN-γ expression was slightly downregulated in the first 90 minutes of TCR stimulation and was significantly upregulated when the cells were stimulated for 100 minutes. Interestingly, we found that the kinetics of c-Rel transcription were similar to those of IFN-γ transcription (Figure 5D, right). In contrast, transcrip-
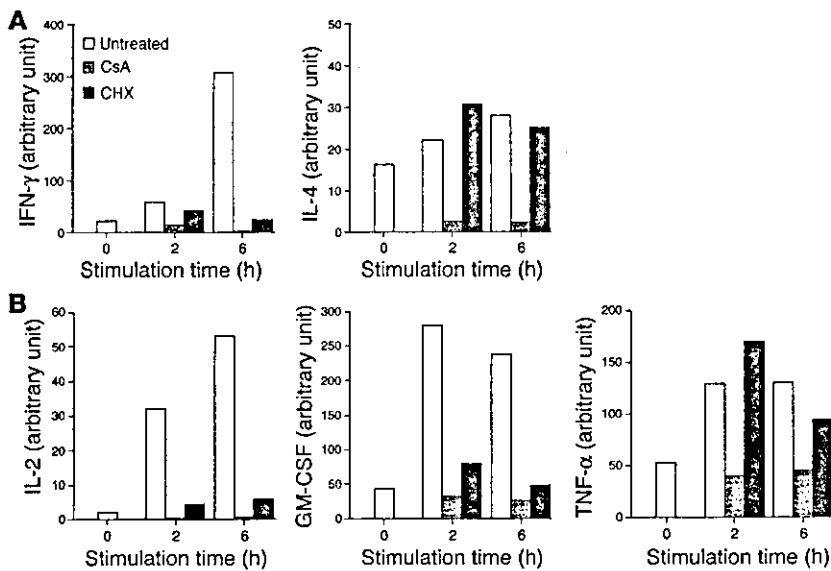
Figure 4
Differential sensitivity to CsA and CHX for transcriptional upregulation of *IFN-γ*, *IL-4*, and other cytokines. (**A**) Sorted NKT cells were pretreated with CsA (1 μg/ml) or with CHX (10 μg/ml) or without either reagent for 10 minutes and were then stimulated with immobilized mAb to CD3 for the indicated periods of time. Total RNA was extracted from each sample and analyzed for the relative amount of transcript of *IFN-γ* or *IL-4*. Data are presented as the amount of transcript in each sample relative to GAPDH. (**B**) Sorted NKT cells were pretreated with CsA (1 μg/ml) or with CHX (10 μg/ml) or without either reagent as shown in **A**. Total RNA was extracted from each sample and was analyzed for the relative amount of transcripts of *IL-2*, *GM-CSF*, or *TNF-α*. Data are presented as the relative amount of transcript in each sample.

tional activation of *IL-4* became evident 30 minutes after TCR stimulation and the transcript accumulated gradually in proportion to the duration of TCR stimulation. This result further confirmed that NKT cells require a longer TCR stimulus for IFN-γ expression.

Transcription of IFN-γ genes depends on c-Rel expression in NKT cells. To further investigate the functional involvement of c-Rel in the transcription of *IFN-γ* gene in NKT cells, we next examined whether forced expression of wild-type c-Rel or of its loss-of-function mutant could affect IFN-γ production by NKT cells. For this, we used bicistronic retroviral vectors expressing c-Rel along with GFP (pMIG/c-Rel) or a c-Rel dominant negative mutant that lacks the C-terminal transactivation domain but retains an intact Rel homology domain of c-Rel protein (pMIG/c-RelΔTA) (21) (Figure 6A). We infected liver-derived mononuclear cells with either retrovirus and stimulated sorted GFP-positive NKT cells with immobilized mAb to CD3 to analyze cytokine production. Retroviral transduction led to expression of GFP in approximately 10% of NKT cells (Figure 6B). Upon stimulation with mAb to CD3, GFP-positive cells from pMIG/c-Rel-infected cultures showed slightly augmented IFN-γ production compared with that of control pMIG-infected cells (Figure 6C). In contrast, GFP-positive cells from pMIG/c-RelΔTA-infected cultures secreted almost no IFN-γ after TCR stimulation (Figure 6C). These results demonstrate that inhibition of c-Rel function, via the introduction of a mutant form of c-Rel, abolishes IFN-γ production and that functional c-Rel is important for effective production of IFN-γ in activated NKT cells.

Discussion

In this study, we investigated the molecular mechanism for differential production of IFN-γ and IL-4 by activated NKT cells through a comparative analysis using the prototypic NKT cell ligands αGC and OCH. Treatment with αGC induced expression of both IFN-γ and IL-4 simultaneously, but OCH induced selective expression of IL-4 by NKT cells. Furthermore, we demonstrated that the CD1d-associated glycolipids with various lipid chain lengths showed different half-lives for NKT cell stimulation when applied in an endosome/lysosome-independent manner and induced the differential cytokine production by NKT cells in a lipid length–dependent manner. Accordingly, we demonstrated that IFN-γ production by NKT cells required lon-

ger TCR stimulation than did IL-4 production and depended on de novo protein synthesis. An NF-κB family transcription factor gene, the *c-Rel* gene, was inducibly transcribed in αGC-stimulated but not in OCH-stimulated NKT cells. Retroviral transduction of a loss-of-function mutant of c-Rel revealed the functional involvement of c-Rel in IFN-γ production by ligand-activated NKT cells. These results have provided a new interpretation of NKT cell activation — that the duration of TCR stimulation is critically influenced by the stability of each glycolipid ligand on CD1d molecules, which leads to the differential cytokine production by NKT cells.

We have previously demonstrated that administration of OCH consistently suppresses the development of EAE by inducing a Th2 bias in autoimmune T cells and that this Th2 shift is probably mediated by selective IL-4 production by NKT cells in vivo (9). Here we directly evaluated the cytokine profile of OCH-stimulated NKT cells using quantitative PCR analysis. Consistent with the previous assumption, NKT cells stimulated with OCH induced rapid production of IL-4 but led to only marginal induction of IFN-γ, confirming the presumed mechanism for the effect of OCH on EAE and CIA. As the "fold induction" of *IFN-γ* transcript after 1.5 hours of stimulation with αGC in microarray analysis was relatively low (fivefold for liver NKT cells and fourfold for spleen NKT cells) compared with the in vivo data, there are several possibilities to explain these results. First, quiescent transcripts of *IFN-γ* pre-existing in resting Vα14-invariant NKT cells (22) may raise the baseline of signal intensity in samples from untreated animals, resulting in a relative decrease in "fold induction" after glycolipid treatment. Second, detection of *IFN-γ* transcription in αGC-stimulated NKT cells might not be optimal, as injection of αGC induced a rapid elevation in IL-4 with the peak value at 2 hours and a delayed and prolonged elevation in IFN-γ in B6 mice (9). Third, αGC treatment significantly induces transcription of *CD154* (18.0-fold for αGC vs. 5.4-fold for OCH; data not shown), whose promoter has a functional NF-AT binding site and CD28 responsive element (CD28RE) (23, 24). Thus, augmented CD40/CD154 interaction may induce IL-12 expression by APCs, resulting in additional IFN-γ production (25). Finally, NKT cells are not necessarily the only source of IFN-γ after in vivo stimulation with αGC. The "serial" production of IFN-γ by NKT cells and NK cells has been demonstrated (6, 26). In particular, a C-glycoside analog of αGC has

Table 2

Differential gene expression patterns in αGC-treated and OCH-treated murine NKT cells

Common name	GenBank	Liver CD3+NK1.1+ Untreated	αGC 1.5 h	αGC 12 h	OCH 1.5 h	OCH 12 h	Spleen CD3+NK1.1+ Untreated	αGC 1.5 h	αGC 12 h	OCH 1.5 h	OCH 12 h
IFN-γ	K00083	1.0 P	5.0 P	0.3 P	1.2 P	0.1 P	1.0 P	4.0 P	2.3 P	0.7 P	1.0 P
IL-2	m16762	1.0 A	391.4 P	1.2 A	12.3 P	1.3 A	1.0 A	23.4 P	0.2 A	1.0 A	0.3 A
IL-2	K02292	1.0 A	129.6 P	0.6 A	32.8 A	1.1 A	1.0 A	16.1 A	0.7 A	10.7 A	1.5 A
GM-CSF	X03020	1.0 P	38.0 P	0.4 A	4.1 P	0.1 A	1.0 A	15.7 P	1.4 A	2.7 A	2.1 A
IL-4	X03532	1.0 P	276.8 P	2.5 P	47.3 P	0.2 A	1.0 A	364.9 P	35.1 P	38.8 P	4.7 P
IL-4	M25892	1.0 P	38.2 P	0.2 P	7.7 P	0.1 A	1.0 P	69.6 P	7.6 P	9.1 P	1.1 P
IL-4	X03532	1.0 A	34.8 P	3.9 A	9.4 A	1.9 A	1.0 A	2.2 A	4.2 A	1.1 A	0.7 A
IL-13	M23504	1.0 A	993.0 P	1.4 A	56.1 P	1.8 A	1.0 A	140.7 P	12.3 A	19.1 A	2.3 A
TNF-α	D84196	1.0 P	30.8 P	2.1 P	1.7 P	1.2 P	1.0 P	16.5 P	2.5 P	1.8 P	2.6 P
Lymphotoxin A	M16819	1.0 P	6.9 P	0.2 A	1.4 P	0.1 A	1.0 P	2.5 P	1.7 P	1.2 P	0.9 P
IL-1α	M14639	1.0 P	25.1 P	5.6 P	3.1 P	4.4 P	1.0 P	6.7 P	5.8 P	1.1 P	2.7 P
IL-1β	M15131	1.0 P	8.0 P	9.8 P	1.3 P	7.9 P	1.0 P	3.3 P	2.2 P	0.6 P	1.5 P
IL-1RA	L32838	1.0 P	10.9 P	15.2 P	1.1 A	11.3 P	1.0 P	5.3 P	28.0 P	0.9 P	23.4 P
IL-3	K01668	1.0 A	33.2 P	2.6 A	4.7 A	1.2 A	1.0 A	4.0 A	1.1 A	1.4 A	1.7 A
IL-6	X54542	1.0 A	34.8 P	16.5 P	8.8 P	10.7 P	1.0 A	19.1 P	17.8 P	1.8 A	12.2 A

Real-time PCR analyses were conducted for *IFN-γ* and *IL-4* as well as for other selected cytokine genes listed in Figure 4 (data not shown) to confirm the correlation with those obtained from microarray analysis. Each probe was assigned a "call" of present (P; expressed) or "absent" (A; not expressed) using the Affymetrix decision matrix. GenBank, GenBank accession number; *IL-1RA*, *IL-1* receptor antagonist.

recently been shown to induce Th1-type activity superior to that induced by αGC, and IL-12 is indispensable for the Th1-skewing effect of the analog (27), indicating the importance of IL-12 in augmenting IFN-γ production in vivo (14, 28). Interestingly, the C-glycoside analog induces production of IFN-γ and IL-4 by NKT cells less strongly than does αGC at 2 hours after in vivo administration. Given that αGC and C-glycoside analog have the same structure for their lipid tails, they might be expected to have comparable affinity for CD1d molecules, and the slightly "twirled" α-anomeric galactose moiety between C-glycoside and O-glycoside may modulate the agonistic effect of these glycolipids. Furthermore, the C-glycoside is more resistant to hydrolysis in vivo and may have an advantage for effective production of IL-12 by APCs. In fact, OCH induces marginal IL-12 production after in vivo administration (data not shown), which makes it unable to induce IFN-γ production by various cells. Therefore, the beneficial feature of OCH as an immunomodulator is that it does not trigger production of IFN-γ in vivo.

As described previously, NKT cells recognize glycolipid antigens in the context of the nonpolymorphic MHC class I–like molecule CD1d (4). Crystal structure analysis revealed that the mouse CD1d molecule has a narrow and deep binding groove with extremely hydrophobic pockets, A′ and F′ (29). Thus the two aliphatic hydrocarbon chains would be captured by this binding groove of CD1d and the more hydrophilic galactose moiety of αGC or OCH would be presented to TCR on NKT cells. As OCH is an analog of αGC with a truncated sphingosine chain, it could be predicted that truncation of the hydrocarbon chain would make it more unstable on CD1d, which might then affect the duration of TCR stimulation on NKT cells. We demonstrated in this study that OCH detached from the CD1d molecule more rapidly than did αGC after a short-term pulse in which the glycolipids were segregated from the endosomal/lysosomal pathway. Accordingly, we showed that the initiation of IFN-γ production by NKT cells required more prolonged TCR stimulation than was required for IL-4 production. Methods

such as surface plasmon resonance were not appropriate for direct assessment of the interaction between glycolipids and CD1d, possibly because of unpredictable micelle formation and the poor solubility of glycolipids in aqueous solvents (30). The half-life of the interaction of glycolipids and CD1d was reported to be less than 1 minute by surface plasmon resonance (31), contradicting functional assays suggesting a much longer half-life. Therefore, we applied a biological assay to evaluate the stability of these glycolipids on CD1d molecules, as described previously (13).

The characteristics of OCH are somewhat analogous to those of an altered peptide ligand (APL) that has been shown to induce a subset of functional responses observed in intact peptide and, in some cases, induce production of selected cytokines by T cells (32–34). Thus, OCH and possibly other αGC derivatives could be called "altered glycolipid ligands" (AGLs). Although the biological effects of APLs and AGLs could mediate a series of similar molecular events in target cells, it should be noted that APLs and AGLs differ in their "conceptual features." That is, APLs are usually altered in their amino acid residues to modify their affinity for TCRs, whereas AGLs have truncation of their hydrocarbon chain responsible for CD1d anchoring. This paper has highlighted the duration of NKT cell stimulation by CD1d-associated glycolipids as being a critical factor for determining the nature of AGLs for selective induction of cytokine production by NKT cells.

Given that IL-4 secretion consistently precedes IFN-γ production by NKT cells after TCR ligation, we speculated there were critical differences in the upstream transcriptional requirements for the *IFN-γ* and *IL-4* genes in NKT cells. In support of this speculation, CHX treatment specifically inhibited the transcription of *IFN-γ* but not that of *IL-4*. In contrast, transcription of both cytokines was abolished by CsA treatment, indicating that TCR-mediated activation of NF-AT is essential for the production of both cytokines. TCR signal-induced NF-AT activation occurs promptly corresponding to calcium influx (35). Meanwhile, the protein expression of specific
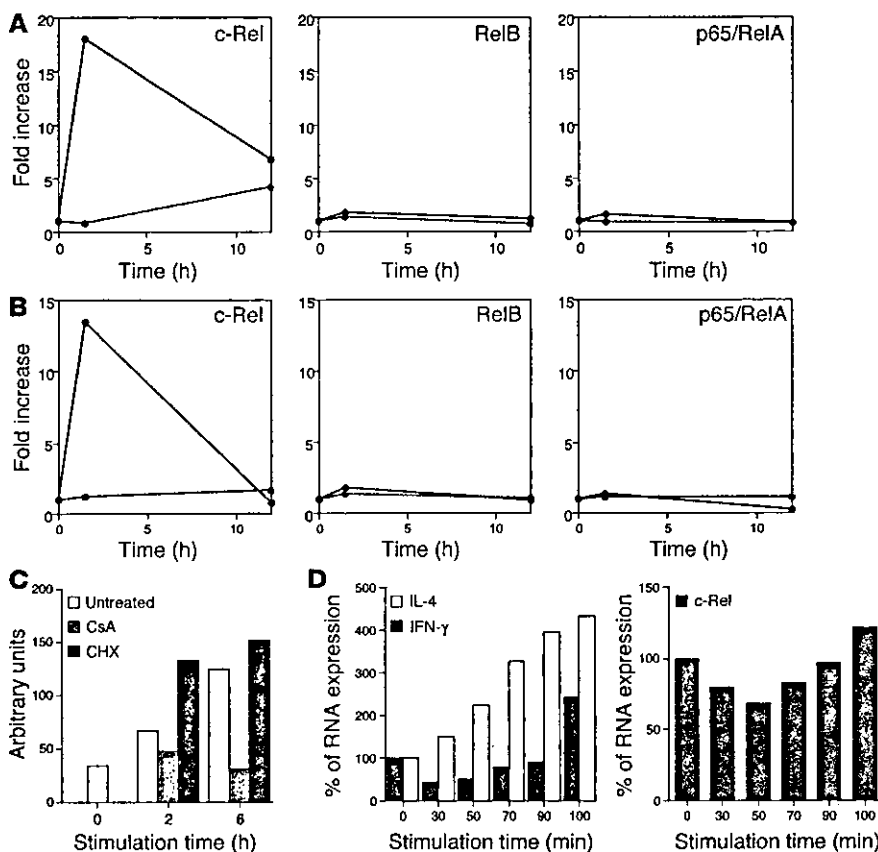
Figure 5
Induction of NF-κB family members in activated NKT cells. (**A**) Plotted values represent data of Affymetrix microarray analysis for the indicated genes. The αGC-stimulated (red lines) or OCH-stimulated (green lines) cells as well as unstimulated liver NKT cells were analyzed at the same time points and the data are presented as the relative value for stimulated NKT cells when the value in NKT cells derived from untreated animals was defined as 1. (**B**) Real-time PCR analysis for the same genes as in **A**. Data are presented as described in Figure 4. (**C**) Sorted liver NKT cells were pretreated with CsA or CHX and were stimulated with immobilized mAb to CD3, and comparative values of c-Rel transcripts relative to GAPDH were determined. (**D**) Sorted liver NKT cells were stimulated with immobilized mAb to CD3 for the indicated periods of time and then were cultured without stimulation for up to a total of 120 minutes after the initial stimulation. Total RNA was extracted from each sample and analyzed for relative amounts of transcripts of *IFN-γ* or *IL-4* (left), or *c-Rel* (right). The amount of RNA derived from unstimulated NKT cells was defined as 100%.

transcription factors takes more time to accomplish. The requirement for prolonged TCR stimulation for initiation of *IFN-γ* transcription may be due to its dependency on specific gene expression.

Recently, Matsuda et al. have shown using cytokine reporter mice that Vα14-invariant NKT cells express cytokine transcripts in the resting state, but express protein only after stimulation (22). We obtained a similar result with our microarray analysis, in that many cytokine transcripts including *IFN-γ* and *IL-4* were detectable in unstimulated NKT cells derived from liver or spleen, because most of them were assigned a "call" of "present" by the Affymetrix decision matrix, which means they were significantly expressed. The mechanism of translation of pre-existing cytokine transcripts after activation of NKT cells remains to be investigated.

Through microarray analysis and real-time PCR, we next identified a member of the NF-κB family of transcription factors, c-Rel, as being a protein rapidly expressed after αGC treatment and possibly responsible for the transcription of *IFN-γ*. Treatment with αGC selectively upregulated *c-Rel* transcription 1.5 hours after stimulation of NKT cells in vivo. OCH treatment, however, showed no induction of *c-Rel* transcription. Although *c-Rel* is transcriptionally upregulated after TCR stimulation of T cells (36), transcription of other NF-κB family members such as *p65/RelA*, *RelB*, *NF-κB1*, and *NF-κB2* was unchanged (data not shown). CsA treatment inhibited c-Rel transcription, but CHX did not, indicating that inducible transcription of c-Rel was directly controlled by TCR signal–mediated activation of NF-AT, which is consistent with a previous report (19). Although the pre-existing NF-κB proteins in general provide a means of rapidly altering cellular responses by inducing the destruction of IκB in order to enable NF-κB to be free for nuclear transloca-

tion and DNA binding, most of the nuclear c-Rel induced after T cell stimulation has been shown to be derived from newly translated c-Rel proteins. In contrast, pre-existing c-Rel scarcely translocates to the nucleus at all (36), indicating that the nuclear induction of c-Rel in T lymphocyte requires ongoing protein synthesis. The retrovirally transduced loss-of-function mutant c-Rel (c-RelΔTA) significantly inhibited transcription of *IFN-γ* genes, indicating the crucial role of c-Rel in their transcription after activation of NKT cells. Although it is possible that the Rel domain of the dominant negative mutant may affect a number of NF-κB dimers, it is unlikely, because IFN-γ production by stimulated NKT cells were CHX sensitive and other NK-κB members were not induced after stimulation in the microarray analysis. Retroviral transduction of wild-type c-Rel into NKT cells resulted in slightly augmented expression of IFN-γ after stimulation. Induction of endogenous c-Rel after in vitro stimulation might reduce the effect of retrovirally introduced c-Rel protein.

Whereas c-Rel has been associated with the functions of various cell types, its role in the immune system was first demonstrated in its involvement in *IL-2* transcription (37), in which it possibly induced chromatin remodeling of the promoter (38). Recently, the promoters for the genes encoding *IL-3*, *IL-5*, *IL-6*, *TNF-α*, *GM-CSF*, and *IFN-γ* were shown to contain κB sites or the κB-related CD28RE. Gene targeting of *c-Rel* in mice revealed that *c-Rel*-deficient T cells have a defect in the production of IL-2, IL-3, IL-5, GM-CSF, TNF-α, and IFN-γ, although expression of some of the cytokines was rescued by the addition of exogenous IL-2 (39, 40). Regarding the involvement of c-Rel in IFN-γ production, the c-Rel inhibitor pentoxyfylline (41) selectively suppresses Th1 cytokine production and EAE induction (42), and transgenic mice expressing the *trans*-dominant form of IκBα have a defect in IFN-γ production and the Th1 response (43). Recently, an elegant study using *c-Rel*-deficient mice revealed *c-Rel* has crucial roles in IFN-γ production by activated T cells and conse-

A pMIG(W)

pMIG(W)/c-Rel
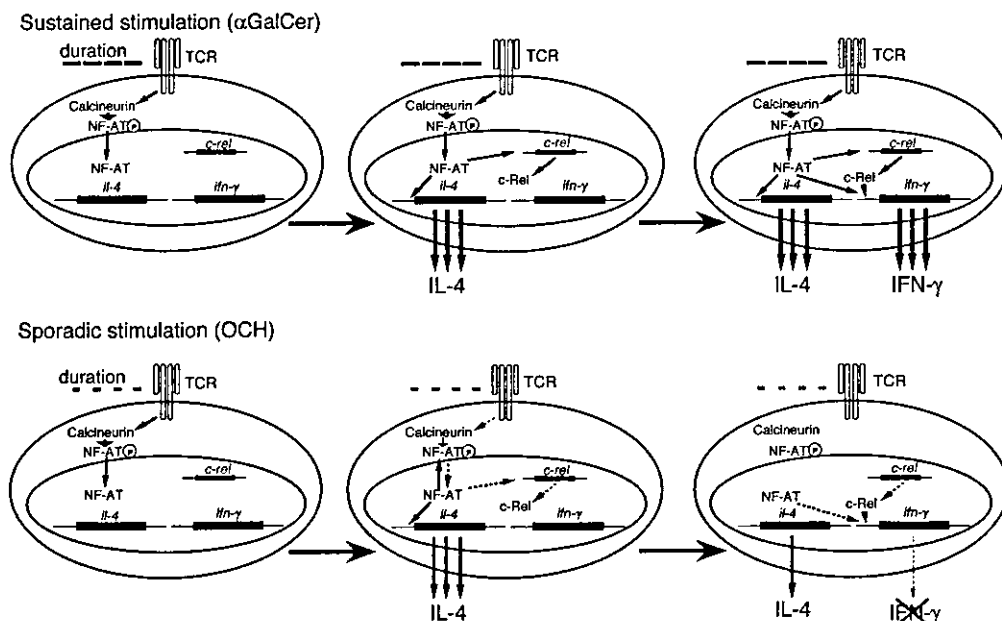
pMIG(W)/c-RelΔTA

B

C
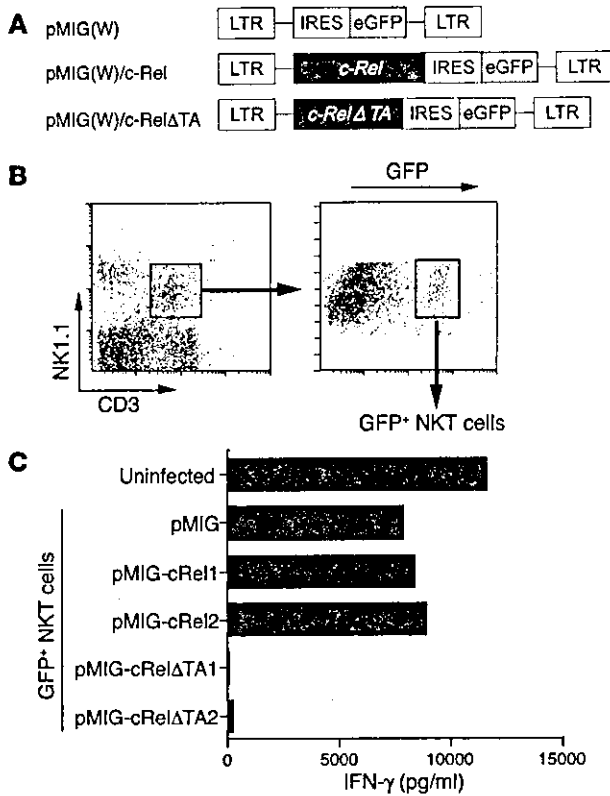
Figure 6

Cytokine production after retroviral transduction of c-Rel or c-RelΔTA into NKT cells. **(A)** DNA fragments encoding wild-type c-Rel or its mutant were cloned into the pMIG(W) bicistronic retrovirus vector. The mutant form of c-Rel (c-RelΔTA) lacks the transactivation domain of the c-Rel protein. LTR, long terminal repeat; IRES, internal ribosome entry site; eGFP, enhanced GFP. **(B)** Flow cytometric identification of cells transfected with the viral vector. Among the NK1.1+CD3+ liver NKT cells identified in the left panel, approximately 10% were GFP positive. The GFP-positive NKT cells were sorted for further analysis. **(C)** IFN-γ production by NKT cells transfected with c-Rel or its dominant negative mutant. The CD3+NK1.1+ NKT cells infected with the viruses were isolated based on their expression of GFP and were stimulated with immobilized mAb to CD3. For transduction of c-Rel or c-RelΔTA into NKT cells, two independent clones of each retroviral vector were used. The level of IFN-γ in the supernatants was measured by ELISA.

cells and that c-Rel plays a crucial role in IFN-γ production as well. NF-AT shows quick and sensitive nucleocytoplasmic shuttling after TCR activation (35). Feske et al. demonstrated that the pattern of cytokine production by T cells was determined by the duration of nuclear residence of NF-AT (44) and that sustained NF-AT signaling promoted IFN-γ expression in CD4+ T cells (45). Considering the structural feature of αGC with longer lipid chain, sustained stimulation by αGC induces long-lasting calcium influx, resulting in sustained nuclear residence of NF-AT, and c-Rel protein synthesis, which enables NKT cells to produce IFN-γ. In contrast, the rather sporadic stimulation by OCH induces short-lived nuclear residence of NF-AT, followed by marginal c-Rel expression, which leaves NKT cells unable to produce IFN-γ (Figure 7). Thus, the kinetic and quantitative differences between αGC and OCH in the induction of transcription factors, such as NF-AT and c-Rel, determine the pattern of cytokine production by NKT cells. As CD1d molecules are nonpolymorphic and are remarkably well conserved among the species, the preferential induction of IL-4 production through NKT activa-

quent Th1 development by affecting the cellular functions of both T cells and APCs (20).Thus, the critical involvement of c-Rel for IFN-γ production in NKT cells is consistent with these findings.

Our results indicate that rapid calcium influx and subsequent NF-AT activation is essential for IFN-γ production by activated NKT

Figure 7

A model for the differential expression of IFN-γ and IL-4 after treatment of NKT cells with αGC or OCH. See text for details.

tion and subsequent Th2 polarization suggest that OCH may be an attractive therapeutic reagent to use for Th1-mediated autoimmune diseases such as multiple sclerosis and rheumatoid arthritis.

Address correspondence to: Sachiko Miyake, Department of Immunology, National Institute of Neuroscience, NCNP, 4-1-1 Ogawahigashi, Kodaira, Tokyo 187-8502, Japan. Phone: 81-42-341-2711; Fax: 81-42-346-1753; E-mail: miyake@ncnp.go.jp.

1. Kronenberg, M., and Gapin, L. 2002. The unconventional lifestyle of NKT cells. *Nat. Rev. Immunol.* 2:557–568.
2. Taniguchi, M., Harada, M., Kojo, S., Nakayama, T., and Wakao, H. 2003. The regulatory role of Vα14 NKT cells in innate and acquired immune response. *Annu. Rev. Immunol.* 21:483–513.
3. Brossay, L., et al. 1998. CD1d-mediated recognition of an α-galactosylceramide by natural killer T cells is highly conserved through mammalian evolution. *J. Exp. Med.* 188:1521–1528.
4. Kawano, T., et al. 1997. CD1d-restricted and TCR-mediated activation of vα14 NKT cells by glycosylceramides. *Science.* 278:1626–1629.
5. Spada, F.M., et al. 1998. CD1d-restricted recognition of synthetic glycolipid antigens by human natural killer T cells. *J. Exp. Med.* 188:1529–1534.
6. Carnaud, C., et al. 1999. Cross-talk between cells of the innate immune system: NKT cells rapidly activate NK cells. *J. Immunol.* 163:4647–4650.
7. Fujii, S.I., Shimizu, K., Smith, C., Bonifaz, L., and Steinman, R.M. 2003. Activation of natural killer T cells by α-galactosylceramide rapidly induces the full maturation of dendritic cells in vivo and thereby acts as an adjuvant for combined CD4 and CD8 T cell immunity to a coadministered protein. *J. Exp. Med.* 198:267–279.
8. Chiba, A., et al. 2004. Suppression of collagen-induced arthritis by natural killer T cell activation with OCH, a sphingosine-truncated analog of α-galactosylceramide. *Arthritis Rheum.* 50:305–313.
9. Miyamoto, K., Miyake, S., and Yamamura, T. 2001. A synthetic glycolipid prevents autoimmune encephalomyelitis by inducing TH2 bias of natural killer T cells. *Nature.* 413:531–534.
10. Burdin, N., et al. 1998. Selective ability of mouse CD1 to present glycolipids: α-galactosylceramide specifically stimulates Vα 14+ NK T lymphocytes. *J. Immunol.* 161:3271–3281.
11. De Silva, A.D., et al. 2002. Lipid protein interactions: the assembly of CD1d1 with cellular phospholipids occurs in the endoplasmic reticulum. *J. Immunol.* 168:723–733.
12. Antonsson, A., Hughes, K., Edin, S., and Grundstrom, T. 2003. Regulation of c-Rel nuclear localization by binding of Ca2+/calmodulin. *Mol. Cell. Biol.* 23:1418–1427.
13. Moody, D.B., et al. 2002. Lipid length controls antigen entry into endosomal and nonendosomal pathways for CD1b presentation. *Nat. Immunol.* 3:435–442.
14. Fujii, S., Shimizu, K., Kronenberg, M., and Steinman, R.M. 2002. Prolonged IFN-γ-producing NKT response induced with α-galactosylceramide-loaded DCs. *Nat. Immunol.* 3:867–874.
15. Akbari, O., et al. 2003. Essential role of NKT cells producing IL-4 and IL-13 in the development of allergen-induced airway hyperreactivity. *Nat. Med.* 31:31.
16. Heller, F., Fuss, I.J., Nieuwenhuis, E.E., Blumberg, R.S., and Strober, W. 2002. Oxazolone colitis, a Th2 colitis model resembling ulcerative colitis, is

mediated by IL-13-producing NK-T cells. *Immunity.* 17:629–638.
17. Leite-de-Moraes, M.C., et al. 2002. Ligand-activated natural killer T lymphocytes promptly produce IL-3 and GM-CSF in vivo: relevance to peripheral myeloid recruitment. *Eur. J. Immunol.* 32:1897–1904.
18. Chen, H., Huang, H., and Paul, W.E. 1997. NK1.1+ CD4+ T cells lose NK1.1 expression upon in vitro activation. *J. Immunol.* 158:5112–5119.
19. Venkataraman, L., Burakoff, S.J., and Sen, R. 1995. FK506 inhibits antigen receptor-mediated induction of c-rel in B and T lymphoid cells. *J. Exp. Med.* 181:1091–1099.
20. Hilliard, B.A., et al. 2002. Critical roles of c-Rel in autoimmune inflammation and helper T cell differentiation. *J. Clin. Invest.* 110:843–850. doi:10.1172/JCI200215254.
21. Carrasco, D., et al. 1998. Multiple hemopoietic defects and lymphoid hyperplasia in mice lacking the transcriptional activation domain of the c-Rel protein. *J. Exp. Med.* 187:973–984.
22. Matsuda, J.L., et al. 2003. Mouse Vα14i natural killer T cells are resistant to cytokine polarization in vivo. *Proc. Natl. Acad. Sci. U. S. A.* 100:8395–8400.
23. Tsytsykova, A.V., Tsitsikov, E.N., and Geha, R.S. 1996. The CD40L promoter contains nuclear factor of activated T cells-binding motifs which require AP-1 binding for activation of transcription. *J. Biol. Chem.* 271:3763–3770.
24. Parra, E., Mustelin, T., Dohlsten, M., and Mercola, D. 2001. Identification of a CD28 response element in the CD40 ligand promoter. *J. Immunol.* 166:2437–2443.
25. Kitamura, H., et al. 1999. The natural killer T (NKT) cell ligand α-galactosylceramide demonstrates its immunopotentiating effect by inducing interleukin (IL)-12 production by dendritic cells and IL-12 receptor expression on NKT cells. *J. Exp. Med.* 189:1121–1128.
26. Smyth, M.J., et al. 2002. Sequential production of interferon-γ by NK1.1+ T cells and natural killer cells is essential for the antimetastatic effect of α-galactosylceramide. *Blood.* 99:1259–1266.
27. Schmieg, J., Yang, G., Franck, R.W., and Tsuji, M. 2003. Superior protection against malaria and melanoma metastases by a C-glycoside analogue of the natural killer T cell ligand α-galactosylceramide. *J. Exp. Med.* 198:1631–1641.
28. Brigl, M., Bry, L., Kent, S.C., Gumperz, J.E., and Brenner, M.B. 2003. Mechanism of CD1d-restricted natural killer T cell activation during microbial infection. *Nat. Immunol.* 4:1230–1237.
29. Zeng, Z., et al. 1997. Crystal structure of mouse CD1: An MHC-like fold with a large hydrophobic binding groove. *Science.* 277:339–345.
30. Cantu, C., 3rd, Benlagha, K., Savage, P.B., Bendelac, A., and Teyton, L. 2003. The paradox of immune molecular recognition of α-galactosylceramide: low affinity, low specificity for CD1d, high affinity for αβ TCRs. *J. Immunol.* 170:4673–4682.
31. Benlagha, K., Weiss, A., Beavis, A., Teyton, L., and

Bendelac, A. 2000. In vivo identification of glycolipid antigen-specific T cells using fluorescent CD1d tetramers. *J. Exp. Med.* 191:1895–1903.
32. Evavold, B.D., and Allen, P.M. 1991. Separation of IL-4 production from Th cell proliferation by an altered T cell receptor ligand. *Science.* 252:1308–1310.
33. Chaturvedi, P., Yu, Q., Southwood, S., Sette, A., and Singh, B. 1996. Peptide analogs with different affinities for MHC alter the cytokine profile of T helper cells. *Int. Immunol.* 8:745–755.
34. Boutin, Y., Leitenberg, D., Tao, X., and Bottomly, K. 1997. Distinct biochemical signals characterize agonist- and altered peptide ligand-induced differentiation of naive CD4+ T cells into Th1 and Th2 subsets. *J. Immunol.* 159:5802–5809.
35. Zhu, J., and McKeon, F. 2000. Nucleocytoplasmic shuttling and the control of NF-AT signaling. *Cell. Mol. Life Sci.* 57:411–420.
36. Venkataraman, L., Wang, W., and Sen, R. 1996. Differential regulation of c-Rel translocation in activated B and T cells. *J. Immunol.* 157:1149–1155.
37. Ghosh, P., Tan, T.H., Rice, N.R., Sica, A., and Young, H.A. 1993. The interleukin 2 CD28-responsive complex contains at least three members of the NF κ B family: c-Rel, p50, and p65. *Proc. Natl. Acad. Sci. U. S. A.* 90:1696–1700.
38. Rao, S., Gerondakis, S., Woltring, D., and Shannon, M.F. 2003. c-Rel Is required for chromatin remodeling across the IL-2 gene promoter. *J. Immunol.* 170:3724–3731.
39. Gerondakis, S., et al. 1996. Rel-deficient T cells exhibit defects in production of interleukin 3 and granulocyte-macrophage colony-stimulating factor. *Proc. Natl. Acad. Sci. U. S. A.* 93:3405–3409.
40. Kontgen, F., et al. 1995. Mice lacking the c-rel proto-oncogene exhibit defects in lymphocyte proliferation, humoral immunity, and interleukin-2 expression. *Genes Dev.* 9:1965–1977.
41. Wang, W., Tam, W.F., Hughes, C.C., Rath, S., and Sen, R. 1997. c-Rel is a target of pentoxifylline-mediated inhibition of T lymphocyte activation. *Immunity.* 6:165–174.
42. Rott, O., Cash, E., and Fleischer, B. 1993. Phosphodiesterase inhibitor pentoxifylline, a selective suppressor of T helper type 1- but not type 2-associated lymphokine production, prevents induction of experimental autoimmune encephalomyelitis in Lewis rats. *Eur. J. Immunol.* 23:1745–1751.
43. Aronica, M.A., et al. 1999. Preferential role for NF-κ B/Rel signaling in the type 1 but not type 2 T cell-dependent immune response in vivo. *J. Immunol.* 163:5116–5124.
44. Feske, S., Draeger, R., Peter, H.H., Eichmann, K., and Rao, A. 2000. The duration of nuclear residence of NFAT determines the pattern of cytokine expression in human SCID T cells. *J. Immunol.* 165:297–305.
45. Porter, C.M., and Clipstone, N.A. 2002. Sustained NFAT signaling promotes a Th1-like pattern of gene expression in primary murine CD4+ T cells. *J. Immunol.* 168:4936–4945.

—91—

Another View of T Cell Antigen Recognition: Cooperative Engagement of Glycolipid Antigens by Va14Ja18 Natural TCR[1]

Aleksandar K. Stanic,* R. Shashidharamurthy,* Jelena S. Bezbradica,* Naoto Matsuki,*
Yoshitaka Yoshimura,* Sachiko Miyake,[†] Eun Young Choi,[‡] Todd D. Schell,[§] Luc Van Kaer,*
Satvir S. Tevethia,[§] Derry C. Roopenian,[‡] Takashi Yamamura,[†] and Sebastian Joyce[2]*

Va14Ja18 natural T (iNKT) cells rapidly elicit a robust effector response to different glycolipid Ags, with distinct functional outcomes. Biochemical parameters controlling iNKT cell function are partly defined. However, the impact of iNKT cell receptor β-chain repertoire and how α-galactosylceramide (α-GalCer) analogues induce distinct functional responses have remained elusive. Using altered glycolipid ligands, we discovered that the Vb repertoire of iNKT cells impacts recognition and Ag avidity, and that stimulation with suboptimal avidity Ag results in preferential expansion of high-affinity iNKT cells. iNKT cell proliferation and cytokine secretion, which correlate with iNKT cell receptor down-regulation, are induced within narrow biochemical thresholds. Multimers of CD1d1-αGalCer- and αGalCer analogue-loaded complexes demonstrate cooperative engagement of the Va14Ja18 iNKT cell receptor whose structure and/or organization appear distinct from conventional αβ TCR. Our findings demonstrate that iNKT cell functions are controlled by affinity thresholds for glycolipid Ags and reveal a novel property of their Ag receptor apparatus that may have an important role in iNKT cell activation. *The Journal of Immunology*, 2003, 171: 4539–4551.

Fundamental to the initiation of a cellular immune response is cell-to-cell communication through receptor triggering and the dynamic formation of an immunological synapse. Central to this process is the interaction between the Ag and its cognate receptor, which relays the specificity of recognition. Although much has been learned regarding the interactions between peptide Ags and their cognate TCR, comparatively little is known about the recognition of CD1-restricted glycolipid Ags by specific T cells.

Va14Ja18 natural T (iNKT)[3] cells are a unique subset of CD1d1-restricted T lymphocytes whose invariant α-chain preferentially pairs with Vb8.2 β-chain and less commonly with Vb7. Remarkably, in vivo iNKT cell activation through the TCR results in rapid (i.e., within 60–90 min) and robust IL-4 response and a spectrum of Th1 and Th2 cytokines (reviewed in Ref. 1). In striking contrast, conventional T lymphocytes require up to a day to produce significant amounts of cytokines in response to Ag.

The natural Ag recognized by iNKT cells remains unknown. A variety of CD1d-positive cells activate freshly isolated thymic iNKT cells and derived hybridomas without the addition of any

exogenous Ag (2–6), which suggests the recognition of self-Ags. Moreover, presentation of self-Ags requires CD1d trafficking through the late endosomes/lysosomes (3, 4, 7–9). The recognition of α-galactosylceramide (αGalCer) and α-glucosylceramide by iNKT cells (10–14) suggests a glycosphingolipid nature of the elusive Ags. Although αGalCer is a nonphysiological Ag, our recent studies indicate that it may be a very close mimic of at least one natural iNKT cell ligand (15). Consistent with this conclusion is the fact that αGalCer and/or its close analogue OCH, with a shortened long-chain sphingosine base and acyl chain, exhibit immunopharmacological effects in vivo. Thus, αGalCer acts like an adjuvant enhancing immunity to malaria and other infectious pathogens (16). Furthermore, αGalCer and/or OCH can prevent autoimmune diseases in mouse models of type I diabetes and multiple sclerosis (17–21). Interestingly, the ability of OCH to induce IL-4 alone and no IFN-γ appears to underlie its pharmacological action (19). Thus, delineating the biochemical parameters of Va14Ja18 TCR/Ag interactions is of paramount pharmacological significance.

Interactions of soluble Ag receptors of conventional T cells with cognate Ags are of low affinity (0.1–50 μM) and relatively fast dissociation half-life ($t_{1/2}$ = 10–50 s) (22–25). Va14Ja18 TCR of an iNKT cell hybridoma has been demonstrated to interact with αGalCer-loaded CD1d1 with relatively high affinity (0.2 μM) and very long half-life ($t_{1/2}$ = 175 s) (26). The high-avidity interaction of Va14Ja18 TCR with CD1d1-αGalCer dimer appears to be influenced by TCR β-chain repertoire (27). Recent studies have implicated both optimal dwell time (28) and affinity (29) of TCR-Ag interaction as critical determinants of T cell sensitivity and activation. Furthermore, interactions of conventional TCR with Ag are thought to be stabilized by CD4 and CD8 coreceptors (30–32). Long dwell time of Va14Ja18 TCR/CD1d1-αGalCer interaction (26) appears counterintuitive to the optimal dwell-time requirements for T cell activation. Because iNKT cells might not use coreceptors during Ag engagement, this interaction might require

intrinsically high affinity and long dwell time for activation of this T cell subset.

Ag recognition by conventional T cells entails self-nonself discrimination. Thus, T cells are tuned to extraordinarily sensitive recognition of foreign Ags (on the order of 20–100 molecules per cell) and base activation decisions on affinity and dwell time (23, 24, 28, 29). Considering that a large body of evidence indicates that iNKT cells recognize self-Ag, a paradox ensues. How is it that iNKT cells are not continually activated by very small amounts of self-Ag presented on APCs in vivo? Self-Ag recognition must be finely tuned to prevent iNKT cell activation during physiological conditions, but to rapidly respond to disturbances in cellular physiology. In other words, iNKT cells need to be very sensitive to modest changes in self-Ag concentration. In biological systems, this kind of fine-tuning is often achieved by cooperative ligand engagement. Cooperativity itself is defined as a positive or negative change in multimeric receptor affinity for ligand following primary and subsequent subunit binding events. Thus, positive cooperativity permits disproportionately sensitive ligand engagement by multimeric receptors, resulting in an almost digital off-on response (33). A form of cooperativity in conventional T cell Ag recognition is afforded by coreceptor-mediated stabilization of TCR-Ag interaction in the immunological synapse. How iNKT cells substitute for coreceptor usage and yet remain unresponsive to low levels of self-Ag remains unknown. Initial report of CD1d1-αGalCer tetramers demonstrated that an iNKT cell hybridoma engages Ag with a Hill coefficient of 4.5, which was interpreted to signify the tetravalency of CD1d1-αGalCer tetramers. Hill coefficient depends on valency but is always lower than the number of binding sites of the multimer (i.e., lower than four for any tetrameric molecule) (34). Because the Hill equation used to calculate the Hill coefficient was not provided in the first (35), how the value of 4.5 was obtained remains elusive.

Several questions regarding CD1d1-lipid/TCR interactions remain: Are there affinity and concentration thresholds for the induction of distinct iNKT cell responses? Does the TCR β-chain repertoire impact iNKT cell Ag reactivity in vivo? Does cooperativity play a role in iNKT cell receptor-Ag interactions? In studies relevant to these questions, we demonstrate that the avidity thresholds for iNKT cell receptor determine sensitivity for glycolipid Ag recognition. Despite the invariant nature of the TCR α-chain, TCR β-chain usage by iNKT cells critically impacts the specificity and the avidity for glycolipid Ags. Furthermore, when responding to a suboptimal affinity ligand, high relative avidity iNKT cells are selected. Interestingly, iNKT cell receptor appears to have structure and/or organization distinct from other αβ TCR and engages Ag cooperatively. Taken together, these features of iNKT cell receptor permit sensitive self-Ag recognition and determine their functional outcomes.

Materials and Methods

Mice

Experiments with B6-*Ja18* [36] (a gift from M. Taniguchi (University of Chiba, Chiba, Japan)), B6.129-*CD1d1* [37], and C57BL/6 (The Jackson Laboratory, Bar Harbor, ME) were in compliance with the regulations of the Institutional Animal Care and Use Committee of Vanderbilt University.

Cell lines and hybridomas

CTL clones and hybridomas (generously provided by A. Bendelac (Princeton University, Princeton, NJ) and K. Hayakawa (Fox Chase Cancer Center, Philadelphia, PA)) have been described (38–41).

NKT cell enrichment

C57BL/6 thymocytes and splenocytes reacted with anti-CD161-PE were separated with anti-PE magnetic microbeads using an automated sorter (Miltenyi Biotec, Auburn, CA). Samples were typically >95% CD161^{+}.

Antigens

Glycolipids (12, 19) and peptides (38, 39) have been described. Kirin Brewery (Gumma, Japan) generously provided αGalCer. SV40 T Ag-derived epitope IV (VVYDFLKL), H28 (ILENFPRL), and H60 (LTFNYRNL) peptides were synthesized by F-moc chemistry at the Macromolecular Core Facility (Pennsylvania State University).

Generation of multimers

Preparation of CD1d1-glycolipid (15) and H2K[b]-peptide tetramers (27, 28) has been described. Dimers of CD1d1 (custom order; BD PharMingen, San Diego, CA) and H2K[b] (DimerX; BD PharMingen) are dimeric owing to their fusion to IgG1 H chains. To obviate the potential for artifacts induced by detection mediated via a fluorochrome-conjugated secondary Ab, the dimers were Alexa Fluor 647- or PE-conjugated via Fab specific for the Fc portion of IgG1 (anti-mouse IgG1 Alexa Fluor 647 and PE Zenon kits; Molecular Probes, Eugene, OR). Every batch of tetramer generated was tested for complete loading of αGalCer and its analogues by glycolipid titration loading and testing by reaction with the best characterized iNKT hybridoma N38-2C12.

Flow cytometry

All Abs were from BD PharMingen unless otherwise stated. Tetramer-stained Va14Ja18 iNKT hybridomas (N37-1H5a, Vb8.2Jb2.6; N38-2C12, Vb8.2Jb2.5; N38-3C3, Vb8.2Jb2.2; and DN32.D3, Vb8.2Jb2.4) were also labeled with anti-TCR Cβ-PE (H57-597). NKT cell-enriched thymocytes and splenocytes with anti-NK1.1-PE (PK136), and anti-TCR Cβ-FITC. CTL clones (SV40 epitope IV-specific 2168T as well as minor histocompatibility (mH) Ag-specific SPH60, BH60, and SPH28) reacted with tetramers were also stained with anti-CD8α-FITC. Samples were analyzed using FACSCalibur and CellQuest, version 3.0 (BD Biosciences, Franklin Lakes, NJ) as well as FlowJo 4.2 (Tree Star, San Carlos, CA).

Determination of relative avidity (K_{av})

Equilibrium (>2 h) binding experiments were performed using increasing tetramer concentrations in 100 μl of PBS containing 2% FCS (Invitrogen, Carlsbad, CA) and 0.05% NaN$_3$ at 4°C, to prevent capping and internalization of the TCR. K_{av} was calculated from specific mean fluorescence intensity (MFI; difference between total MFI at a defined tetramer concentration and background MFI derived from ligand-free tetramer binding to the same cells) using nonlinear regression analysis fitted to classical Michaelis-Menten kinetics (Prism 3.02; GraphPad Software, San Diego, CA). MFI (% maximum) shown in the relevant figures is based on V_{max} calculated from nonlinear regression analysis of the data for adequate graphical representation. This permits easy and reliable comparison of data generated in different experiments. Nonlinear Michaelis-Menten regression analysis was preferred, because Scatchard transformation, which uses linear regression, amplifies any variation of the data from the linear curve. That notwithstanding, the results from the Michaelis-Menten kinetics were confirmed by using classical Scatchard transformations to derive the K_{av} (42).

Determination of off-rates

T cells were labeled with 50 μg/ml H2K[b]-peptide or 10 μg/ml CD1d-glycolipid tetramers, respectively, incubated at 4°C for 3 h, and washed extensively. Cells were also stained with 10 μg/ml anti-TCR Cβ-FITC to monitor TCR levels. Following initial tetramer binding, 10[6] cells were chased in 3 ml of buffer with rocking at 4 or 37°C for the indicated time periods and analyzed by flow cytometry.

Measurement of in vivo and in vitro cytokine response

Mice were injected i.v. with the indicated concentrations of glycolipids diluted in PBS from a 220 μg/ml stock solution in vehicle (0.5% v/v polysorbate and 0.9% w/v NaCl). Controls were injected with corresponding dose of vehicle. After 90 min, IL-2, IL-4, IL-13, CSF-2, IFN-γ, and TNF-α in control and immune sera were measured by ELISA using Abs and methods that we have described previously (43).

TCR down-regulation and in vitro expansion

Bulk C57BL/6 splenocytes were incubated for the indicated amounts of time with increasing concentrations of glycolipid Ags. Following stimulation, iNKT cell receptor level was determined by flow-cytometric analysis

following staining with CD1d1-αGalCer tetramer, anti-TCRβ Ab, within electronically gated B220 and CD8-negative lymphocytes. In other experiments, Ags were first equilibrium-loaded overnight onto B6.129-*Tcra*$^{o/o}$ splenocytes, and then mixed with C57BL/6 splenocytes magnetically depleted of MHC class II-positive cells. To directly evaluate iNKT cell division during culture, splenocytes were labeled with 2 μM CFSE (Molecular Probes) in PBS for 8 min at room temperature, followed by quenching with cold FCS and washing with ice-cold RPMI 1640 supplemented with 10% FCS before culture. Evaluation of iNKT cell proliferation was performed by multiplying the percentage of iNKT cells determined by flow cytometry with the total cell number.

Cell-free Ag dissociation assay

Soluble mouse CD1d1 was Ni-affinity purified, as described (44), and bound to ELISA plates at a concentration of 10 μg/ml. Following binding at 4°C for 18 h and blocking of unbound sites with 2% FCS, plate-bound soluble mouse CD1d1 was loaded with 0.1 μM lipids for 12 h at 37°C. After removing excess lipids, the Ag was allowed to dissociate for the indicated times at 37°C. The wells were washed again, and ~5 × 10⁴ hybridoma cells were added to each well. Controls included wells bound with 2 μg/ml anti-CD3ε (positive) or with 5 μg/ml BSA (negative) loaded with 1 μg/ml αGalCer. IL-2 secreted upon activation was monitored by ELISA. Data are presented as the percentage of maximum activation.

Determination of Hill coefficient

Hill coefficient was determined from epitope titration experiments. Briefly, CD1d1 and H2K^b-H28 tetramers or dimers were loaded with increasing amounts of glycolipid ligand or peptide epitopes, respectively. Note that H2K^b tetramers were initially folded with H28-derived epitope, a peptide with low affinity for H2K^b, allowing rapid and efficient ligand exchange (Y. Yoshimura and S. Joyce, unpublished data). Glycolipid and peptide loading occurred at 37°C and room temperature, respectively, for 16–18 h.

Hill curve was derived from data transformation; fractional saturation (Ys) of the receptor was determined as the ratio of specific MFI to maximum MFI (V_{max}) at a defined ligand concentration and plotted against the concentration of added ligand (glycolipid or peptide). Linear graph of logarithmic roots of the values for the *x*- and *y*-axes were used to determine the slope of the Hill curve revealing the Hill coefficient (34).

Results

The CD1d1-αGalCer/Val4Ja18 TCR interaction has high relative avidity

There are a number of different methods available to assess the kinetics and extent of ligand-receptor interactions. Biophysical methods using purified recombinant molecules have been extremely useful in the study of a variety of immunological receptors (45–47). That notwithstanding, methods that examine molecules on living cells are particularly powerful (24, 26, 28, 48, 49). To gain insight into the parameters that govern the binding interactions of the CD1d1 ligand to the specialized TCR of iNKT cells required for their activation, we first determined the K_{av} (measured affinity of tetrameric Ags for the cognate TCR) between tetrameric CD1d1-glycolipid Ag and its receptor on live cells. For comparison, the K_{av} of peptide Ags for the TCR expressed by recently activated CD8$^+$ T lymphocyte (CTL) clones specific for two H2K^b-restricted mH (H60 and H28 (27)) Ags and a viral (SV-40 T Ag-derived epitope IV (39)) Ag was measured. The comparison with class I-restricted Ags was used, because iNKT cells reflect memory/activated T lymphocyte phenotype similar to CTL clones.

CD1d1-αGalCer tetramer binds Val4Ja18$^+$ but not Val4-negative NKT hybridomas (Fig. 1A). Similarly, H2K^b-peptide tetramers specifically bind their cognate, but not irrelevant, CTL clones (data not shown and Refs. 38 and 39). Nonspecific binding was <5% in all cases (Fig. 1A and data not shown). From the binding isotherms, the K_{av} of Ag-TCR interaction was calculated (see *Materials and Methods*).

Val4Ja18 TCR binds CD1d1-αGalCer with a K_{av} ranging from 7 to 17 nM (Fig. 1B and Table I). TCR of conventional T cells bind H2K^b-peptide tetramers with a wide range of K_{av}, ranging from ~20 to 220 nM (Fig. 1C and Table I). Note that, in this study, the

saturation binding isotherms at equilibrium were derived at 4°C. Whereas the K_{av} values obtained at 4°C may not be the same as those at 37°C, the relationship of the K_{av} between different Ag-TCR interactions remains unaltered (50). Consistent with that reported (50), we also found that the K_{av} determined for two iNKT hybridomas at 4°C (N37-1H5a, 10.5 nM; N38-2C12, 18.8 nM) maintained their avidity relationship at 37°C (N37-1H5a, 39.3 nM; N38-2C12, 65.2 nM).

To obtain a more physiological estimate of the K_{av} between CD1d1-αGalCer and Val4Ja18 TCR, the above binding analysis was extended to NKT cell-enriched thymocytes and splenocytes. The K_{av} of CD1d1-αGalCer for Val4Ja18 TCR of live NKT cells (Fig. 1D and Table I) is similar to that observed with iNKT hybridomas (B and Table I). Taken together, the K_{av} of the CD1d1-αGalCer-Val4Ja18 TCR engagement is similar to or higher than that of immunodominant peptide Ag-TCR interaction.

Glycolipid Ag-Val4Ja18 TCR interaction is long-lived

Functional T cell responses following Ag recognition have been correlated with the dwell time, measured as the $t_{1/2}$ of ligand engagement by its receptor (28, 49, 51, 52). We found that the $t_{1/2}$ of glycolipid Ag/Val4Ja18 TCR is long, lasting between 10 and 40 min (Fig. 1E, top two panels; Table I), which is longer than the $t_{1/2}$ observed for peptide Ag/TCR interactions investigated (Fig. 1E, bottom panel; Table I). Hence, the off-rate of CD1d1-αGalCer/TCR interaction on the surface of intact NKT cells appears quantitatively distinct from that of conventional T lymphocytes.

Our data are consistent with previously published reports (28, 53) for studies of peptide-Ag-specific T cells. Due to the manner in which our experiments were performed and analyzed, the data may appear inconsistent with recent dwell-time measurements between CD1d1-αGalCer and iNKT cell receptors (26). Specifically, we did not use anti-CD1d1 or anti-MHC Abs in our experiments, and CD1d1-lipid or MHC-peptide levels detected postchase were not normalized to prechase reacted anti-TCRβ levels. Abs to MHC molecules added during the chase period prevent the dissociating monomers from reassociating with their receptor (49). In our experiments, $t_{1/2}$ of H60 tetramer for cognate TCR determined in the absence (9 ± 0.01 min; see Table I) or presence of an H2K^b-reactive Ab. EH144 (2–10 min; *n* = 5), was similar. Likewise, $t_{1/2}$ of CD1d1-αGalCer tetramers for cognate iNKT cell receptor determined in the absence (9.8 ± 0.9 min; *n* = 5) or presence of 100 μg/ml CD1d1-reactive Ab 1B1 (17.6 ± 7.4 min; *n* = 2) was similar. It should also be noted that, unlike MHC class II, which is not expressed by mouse T cells, MHC class I and CD1d1 are expressed by T lymphocytes. The use of anti-class I or anti-CD1d1 has the potential to cross-link the dissociating tetramer to the T cells, thereby skewing the data toward increased dwell time. Hence, the comparative off-rate measurements were performed in the absence of Abs.

We also found that the TCR levels on iNKT cells and CTL at time zero and at 120 min of chase were similar when they were stained with anti-TCRβ Ab postchase (data not shown). In contrast, prestaining with anti-TCRβ resulted in a significant loss of TCRβ staining during chase, most likely due to the $t_{1/2}$ of anti-TCRβ Ab and cell surface TCR interaction. Thus, we chose not to normalize the remaining CD1d1-αGalCer tetramer bound postchase to prechase reacted anti-TCRβ staining, as described in published reports (28, 53). Nevertheless, our results are consistent with the conclusion that iNKT cell receptor interaction with CD1d1-presenting glycolipid Ag exhibits longer dwell time than that of CTL receptor interaction with peptidic Ags (26).

FIGURE 1. Biochemical features of glycolipid Ag/ Va14Ja18 TCR and peptide Ag/TCR interactions. *A*, Ag-free and αGalCer-loaded CD1d1 tetramer were reacted with Va14-negative or iNKT hybridomas to determine the specificity of the reagent. *B–D*, Saturation binding isotherms were generated by reacting the indicated concentrations of CD1d1-αGalCer tetramers with four iNKT hybridomas (N37-1H5a, Vb8.2Jb2.6; N38-2C12, Vb8.2Jb2.5; N38-3C3, Vb8.2Jb2.2; and DN32.D3, Vb8.2Jb2.4) (*B*) or NKT cell-enriched thymocytes and splenocytes (*D*). Similar isotherms were generated using the indicated concentrations of H2K[b]-peptide tetramers in a reaction with specific CTL clones (SV40 epitope IV-specific 2168T as well as mH Ag-specific SPH60, BH60 and SPH28) (*C*). All binding reactions were performed at 4°C in the presence of sodium azide to prevent ligand-induced capping and TCR internalization. Specific MFI in *B–D* measured by flow cytometry are represented as a fraction of maximum binding. K_{av} was calculated using the Michaelis-Menten equation (see *Materials and Methods*). *E*, To determine the $t_{1/2}$ of Ag-receptor binding, the indicated T cells were reacted with specific tetrameric Ag. After extensive washes, the dissociation of Ag from cells during the chase was monitored by flow cytometry. Specific MFI is represented as a fraction of that detected at the beginning of chase.
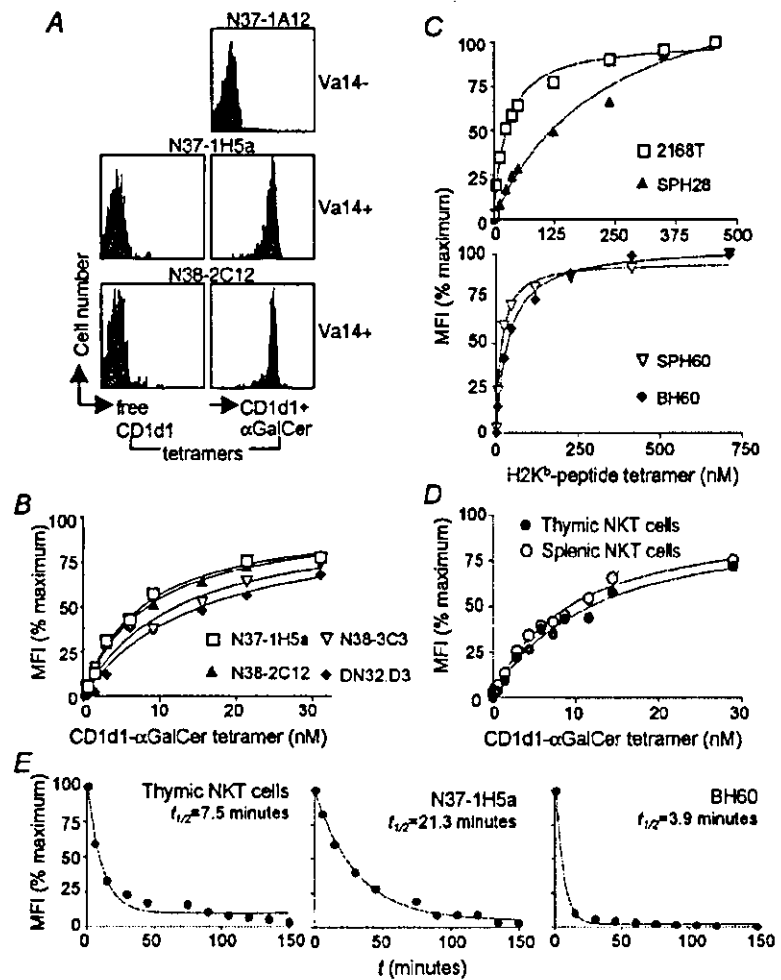
TCR β-chain repertoire of iNKT cells impacts Ag specificity and the K_{av} of their interaction

Altered glycolipid ligands derived from αGalCer elicit distinct functional responses from iNKT cells in vivo and in vitro (19). Recently, the TCR β-chain repertoire of iNKT cells was implicated in high-affinity dimeric CD1d1-αGalCer binding; the

Vb8.2^{+} iNKT cells have higher affinity for Ag than those that express Vb7 (27). Differences in TCR β-chain repertoire and/or the affinity for altered glycolipid ligands could explain the differential Ag specificity and functional outcomes. Tetramers of CD1d1-αGalCer and its analogues OCH, 3,4D, and NH were generated concurrently under saturating conditions. Tetramers of

Table I. *Kinetic parameters of Ag-TCR interactions*

				Hill Coefficient (h)[b] ± SEM (n)	
T Cell	Reactivity[a]	K_d (nM)[b] ± SEM (n)[c]	$t_{1/2}$ (min at 37°C)[b] ± SEM (n)	Tetramer	Dimer
iNKT hybridomas/CD1d1-αGalCer					
N37-1H5a	CD1d1 + self lipid	7.5 ± 0.3 (3)	19.1 ± 1.3 (5)	2.8 ± 0.4 (3)	
N38-2C12	CD1d1 + self lipid	8.5 ± 2.0 (4)	42.1 ± 4.3 (5)	2.8 ± 0.3 (3)	1.8 ± 0.2 (2)
DN32.D3	CD1d1 + self lipid	16.8 ± 0.9 (3)	37.3 ± 2.6 (2)	2.6 (1)	
N38-3C3	CD1d1 + self lipid	17.6 ± 3.4 (3)	16.4 ± 1.0 (2)	2.4 (1)	
C57BL/6 iNKT cells/CD1d1-αGalCer					
Thymic	CD1d1 + self lipid	10.7 ± 3.0 (4)	9.8 ± 0.9 (5)	2.5 ± 0.2 (3)	
Splenic	CD1d1 + self lipid	8.8 ± 0.7 (4)	11.4 ± 0.6 (3)	2.7 ± 0.2 (3)	
Conventional CD8^{+} T lymphocytes/H2K[b]-peptide					
2168T	H2K[b] + epiIV	23.9 ± 2.7 (3)	ND	1.1 ± 0.1 (4)	
SPH60	H2K[b] + H60	20.4 ± 2.9 (3)	9.4 ± 0.03 (2)	1.0 ± 0.1 (3)	1.0 ± 0.2 (2)
BH60	H2K[b] + H60	33.4 ± 1.7 (3)	3.9 ± 0.01 (2)	0.9 ± 0.04 (3)	
SPH28	H2K[b] + H28	216.7 ± 9.2 (4)	2.1 ± 0.9 (2)	ND	

[a] The reactivities of all of the T lymphocytes have been described (see *Results* for references).
[b] Calculations of the kinetic parameters are described in *Materials and Methods* (also see *Results* for details).
[c] *n*, Number of experimental values.

FIGURE 2. CD1d1-OCH is recognized with lower K_{av} but similar dwell time compared with CD1d1-αGalCer by a Vb8.1,8.2-skewed iNKT cell repertoire. A, Equimolar quantities (30 nM) of CD1d1-glycolipid tetramers were reacted with a Va14-negative (N37-1A12) or two iNKT (N37-1H5a and N38-3C3) hybridomas, and NKT cell-enriched thymocytes. B, Expression of TCRβ, Vb8.1,8.2, or Vb7 on CD1d1-αGalCer and -OCH tetramer-positive, electronically gated HSA^{low}CD8^{low} thymocytes. C, Expression of TCRβ, Vb8.1,8.2, or Vb7 on CD1d1-αGalCer and -OCH tetramer-positive, magnetically sorted NK1.1$^+$ thymocytes. D and E, Saturation binding isotherms were generated using iNKT hybridomas and NKT cell-enriched thymocytes and splenocytes reacted with the indicated concentrations of CD1d1-αGalCer or -OCH tetramers. Similar binding isotherms were generated using Vb8.1,8.2$^+$ and Vb7$^+$ splenic iNKT cells. From the binding isotherms, K_{av} was calculated as described in Fig. 1. F, $t_{1/2}$ of CD1d1-αGalCer and CD1d1-OCH binding to thymic iNKT cells was determined as described in Fig. 1. Binding reactions in A–E were performed at 4°C in the presence of sodium azide to prevent capping and internalization.
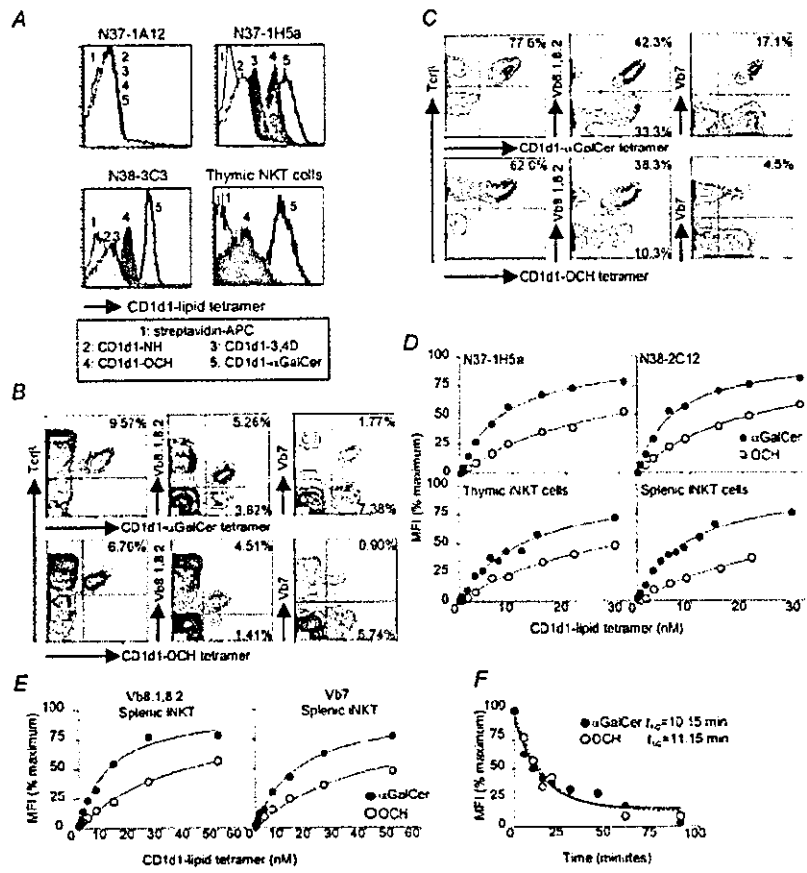
CD1d1-αGalCer, -OCH, and -3,4D have exquisite specificity for iNKT cells (Fig. 2A). However, CD1d1-3,4D (an analogue lacking the two hydroxyl groups at C atoms 3 and 4 of the long-chain base) and especially CD1d1-NH (C atom 2′ amine-modified αGalCer) bind poorly or not at all, respectively, to iNKT hybridomas (Fig. 2A).

To determine the TCR β-chain repertoire of iNKT cells recognizing OCH, bulk (Fig. 2B) and sorted NK1.1$^+$ (C) thymocytes were reacted with CD1d1-αGalCer or CD1d1-OCH tetramers and TCRβ-, Vb8.1,8.2-, or Vb7-specific Abs. Surprisingly, CD1d1-OCH tetramer detected ~30% fewer total iNKT cells compared with CD1d1-αGalCer tetramer (Fig. 2, B and C). Interestingly, a

large majority of CD1d1-OCH tetramer-positive cells expressed Vb8.1,8.2; they reflected 85–90% of CD1d1-αGalCer tetramer-reactive cells (Fig. 2, B and C). Furthermore, Vb8.1,8.2-negative and Vb7$^+$ iNKT cells inefficiently reacted with CD1d1-OCH tetramer (25–50% of CD1d1-αGalCer tetramer-positive cells). However, TCR β-chain usage for CD1d1-3,4D-reactive cells could not be determined, because the MFI of this interaction was very low, and hence, it was difficult to resolve positive from negative staining. These results for the first time directly demonstrate that TCR β-chain repertoire of iNKT cells in vivo impacts their Ag binding. This difference could be a result of differing avidities of the altered

Table II. *Kinetic parameters of glycolipid Ag analogue/TCR interactions*

T Cell	K_d (nM) ± SEM (n)[a]			$t_{1/2}$ (min at 37°C)[b] ± SEM (n)		Hill Coefficient (h) ± SEM (n)	
	αGalCer[c]	OCH	3,4D	αGalCer[c]	OCH	αGalCer[c]	OCH
iNKT hybridomas							
N37-1H5a	7.5 ± 0.3 (3)	29.9 ± 0.3 (2)	ND	10.7 ± 3.0 (4)	ND	2.8 ± 0.4 (3)	2.2 ± 0.4 (2)
N38-2C12	8.5 ± 2.0 (4)	22.1 ± 1.7 (2)	ND	42.1 ± 4.3 (5)	ND	2.8 ± 0.3 (3)	2.3 ± 0.4 (2)
C57BL/6 iNKT cells							
Thymic							
TCRβ$^+$	10.7 ± 3.0 (4)	31.2 ± 0.4 (2)	59.5 ± 3.1 (2)	9.8 ± 0.9 (5)	13.0 ± 1.9 (2)	2.5 ± 0.2 (3)	ND
Vb8.1,8.2$^+$	10.5 ± 0.1 (2)	35.7 ± 1.9 (2)					
Vb7$^+$	16.0 ± 0.8 (2)	46.6 ± 1.8 (2)					
Splenic	8.8 ± 0.7 (4)	27.4 ± 10.9 (2)	ND	ND	ND	2.7 ± 0.2 (3)	ND
Splenic C57BL/6 iNKT cells expanded with glycolipid Ag stimulation (96 h)							
αGalCer	9.1 ± 0.4 (2)	44.2 ± 2.9 (2)					
OCH	9.1 ± 0.6 (2)	39.7 ± 7.2 (2)					
3,4D	6.4 ± 0.5 (2)	25.1 ± 1.9 (2)					

[a] n, Number of experimental values.
[b] Calculations of the kinetic parameters are described in *Materials and Methods* (also see *Results* for details).
[c] αGalCer data is the same as presented in Table 1.

lipids for their TCR. Therefore, CD1d1-αGalCer, -OCH, and -3,4D tetramers were used to determine their K_{av} for the TCR. CD1d1-OCH binds iNKT TCR with about 3- to 4-fold lower K_{av} compared with CD1d1-αGalCer, whereas CD1d1-3,4D had a 6-fold lower K_{av} (Fig. 2D and/or Table II).

Considering that the TCR β-chain repertoire of cells recognizing OCH was Vb8.1.8.2 skewed, we hypothesized that TCR β-chain of the iNKT cell receptor impacts K_{av} for Ag. We found that Vb7$^+$ iNKT cells have 50% lower K_{av} for both CD1d1-αGalCer and -OCH compared with Vb8.1,8.2$^+$ iNKT cells (Fig. 2E and Table II). Note that K_{av} determination was performed with Vb7$^+$ cells that detectably bound CD1d1-OCH tetramer, which represented only ~50% of total CD1d1-αGalCer tetramer-reactive Vb7$^+$ iNKT cells. Therefore, the results potentially represent a higher K_{av} than that of the entire Vb7$^+$ iNKT population. Because the dwell time of TCR and Ag interaction correlates with the capacity for T cell activation, the $t_{1/2}$ of CD1d1-αGalCer, and CD1d1-OCH from iNKT cell receptor was determined as described above. The results indicate that both glycolipid Ags have similar dwell times for their cognate receptors (Fig. 2F and Table II). Taken together, the data suggest that the TCR β-chain repertoire and the K_{av} of Ag-receptor interaction, but not the dwell time, might govern distinct functional outcomes from iNKT cells.

iNKT cells recognize OCH and αGalCer in vivo with similar sensitivity

A number of in vitro studies have indicated that iNKT cells recognize CD1d1-αGalCer with nanomolar sensitivity (10–12, 14, 35). Ags with different binding affinity for their TCR activate T cells with distinct activation thresholds (54–58). To determine the sensitivity of effector responses by iNKT cells in vivo, C57BL/6 mice were injected i.v. with αGalCer and OCH, and serum cytokine response was measured after 90 min. CD1d1-restricted NKT cell (B6.129-CD1d1$^{0/0}$)- and iNKT cell (B6-Ja18$^{0/0}$)-deficient mice do not respond to these glycolipids (Fig. 3A), nor do C57BL/6 mice injected with the vehicle used to dissolve the glycolipid Ags (data not shown).

Mice administered 0.5 μg of OCH elicited substantial amounts of IL-2 and IL-4; TNF-α, IL-13, and CSF-2 (GM-CSF) were also detectable within 90 min (Fig. 3A). Administration of 1.0 μg of αGalCer or OCH elicited a robust cytokine response including TNF-α, IL-13, and CSF-2 (Fig. 3A). Note that the observed IFN-γ response is at the very low end of maximum at this early time point. Furthermore, the previously reported differential IFN-γ response to OCH and αGalCer are strikingly apparent only at or after 6 h (19), because that is the time point at which IFN-γ peaks (59). Thus, at early time, αGalCer and OCH are recognized with similar sensitivity in vivo.

Kinetics of CD1d1 loading with αGalCer and OCH explain similar early iNKT cell response in vivo

Activation of T cells is an effect of Ag-TCR engagement and consequent intracellular signaling. T cell activation correlates with the extent of receptor down-regulation due to signal-dependent altered intracellular TCR trafficking (60–62). Surprisingly, iNKT cells respond to αGalCer and OCH with similar early sensitivity (Fig. 3A), despite different equilibrium binding properties of TCR and specific Ag (Fig. 2, D–F, and Table II). To determine the cellular basis of αGalCer and OCH sensitivity, the kinetics and extent of TCR down-regulation following addition of increasing concentrations of αGalCer and OCH to splenocytes in vitro were evaluated. Both αGalCer and OCH down-regulated similar levels of surface TCR within 4–12 h of Ag stimulation (Fig. 3B, top three panels). However, αGalCer was ~10-fold more potent at inducing surface

TCR down-regulation after 24 h of stimulation. Thus, the kinetics of TCR down-regulation reflected the early induced iNKT cell response in vivo.

Two plausible mechanisms can explain the difference observed in early and late iNKT cell responses to αGalCer and OCH. αGalCer, because of its higher K_{av} for Va14Ja18 TCR compared with OCH, is a more potent iNKT cell ligand resulting in more sustained TCR down-regulation and activation. Alternatively, OCH, because of its shortened sphingosine and acyl chains, binds CD1d1 faster than αGalCer, and hence compensates for its low K_{av} and elicits an early iNKT cell response. To distinguish between the two possibilities, B6.129-Tcra$^{0/0}$ splenocytes, which lack T and iNKT cells, were incubated with increasing quantities of αGalCer and OCH for 24 h. They were then used to stimulate C57BL/6 splenocytes depleted of MHC class II-positive cells, after which iNKT cell receptor down-regulation was evaluated. OCH was 10- to 20-fold less efficient in TCR down-regulation compared with αGalCer at all time points tested (Fig. 3C). This result is consistent with the hypothesis that αGalCer and OCH have different kinetics of CD1d1 loading, and that the similar early iNKT cell response to the two Ags in vivo reflects rapid on-rate of OCH compared with αGalCer.

To determine the concentration threshold required for the elicitation of distinct cytokines from iNKT cells by αGalCer and its analogue OCH, C57BL/6 splenocytes were stimulated with increasing concentrations of these glycolipids. The results revealed that IL-2 and IFN-γ response after 48 h (Fig. 3D) required at least 50% iNKT cell receptor down-regulation measured at 24 h (B, bottom panel) and medium Ag concentration threshold of αGalCer and OCH (D). In contrast, secretion of CSF-2 and IL-4 was more sensitive to low concentrations of glycolipid Ags and, hence, responded to low levels of TCR down-modulation (Fig. 3, B and D). In support of our previous report (19), OCH preferentially induced an IL-4 response, whereas 50-fold higher concentration of OCH was required to produce an IFN-γ response similar to that induced by αGalCer (Fig. 3D). Thus, the secretion of cytokines by iNKT cells follows a hierarchical Ag response pattern, with higher avidity and higher concentrations required for secretion of IFN-γ and IL-2 compared with both low avidity and low concentration for CSF-2 and IL-4.

To fully understand the properties of CD1d1-OCH interaction, we used a cell-free Ag presentation assay to determine its dissociation kinetics. Plate-bound soluble CD1d1 was loaded with equimolar quantities of αGalCer or OCH. After removing unbound lipid, the complexes were allowed to dissociate for varying time periods at 37°C. The $t_{1/2}$ of Ag-CD1d1 complex was monitored by its ability to activate iNKT cell hybridomas. OCH interaction with CD1d1 was more labile, because it dissociated faster than αGalCer from CD1 (Fig. 3E). Thus, similar early sensitivity of iNKT cells to αGalCer and OCH in vivo reflects the differences in the kinetics of their interaction with CD1d1 and also the differences in their equilibrium parameters of TCR engagement.

Activation of iNKT cells by 3,4D in vitro causes selective expansion of high-avidity clones

The altered lipid ligand, 3,4D, engages the iNKT cell receptor, albeit with low K_{av} compared with αGalCer and OCH (Fig. 2B and Table II), and elicits a weak cytokine response in vivo (19). To elucidate the biochemical basis of this weak response, the proliferative capacity of iNKT cells to Ag engagement was determined in vitro by CFSE dye dilution assay. After stimulation of splenocytes with Ags for 96 h, iNKT cells were costained with CD1d1-αGalCer tetramer and TCRβ-specific Ab. At high concentration (575 nM), αGalCer, OCH, and 3,4D induced extensive iNKT cell
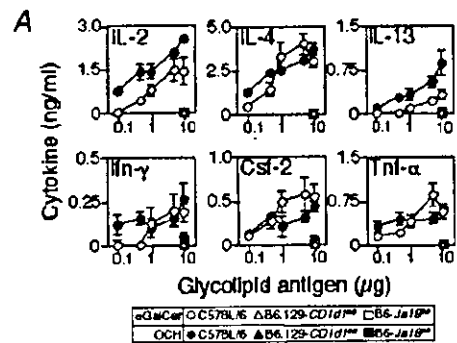
FIGURE 3. Kinetics of CD1d1 loading with αGalCer and OCH explain similar early iNKT cell response in vivo to the two glycolipids. *A*, C57BL/6 mice or control B6.129-*CD1d1*[G/G] and B6-*Ja18*[G/G] mice were injected i.v. with the indicated concentrations of αGalCer, OCH, or vehicle. After 90 min, serum cytokines were monitored. Background cytokine level (<3%) elicited by vehicle-treated mice was subtracted from the Ag-treated response. The data represent cytokine responses (±SE) elicited by four individual mice in two identical experiments. *B*, Val14Ja18 TCR down-regulation was monitored at the indicated time points following addition of αGalCer or OCH to C57BL/6 splenocytes. iNKT cell receptor level was determined by flow-cytometric analysis following reaction with CD1d1-αGalCer tetramer and anti-TCRβ Ab, within electronically gated B220 and CD8-negative lymphocytes. *C*, Val14Ja18 TCR down-regulation was monitored following reaction of C57BL/6 splenocytes magnetically depleted of MHC class II-positive cells with B6.129-*Tcra*[G/G] splenocytes equilibrium loaded with Ag overnight. *D*, Cytokines elicited by C57BL/6 splenocytes were monitored 48 h following addition of indicated quantities of αGalCer or OCH in vitro by sandwich ELISA. *E*, The dissociation of αGalCer and OCH from plate-bound soluble CD1d1 was monitored after removing excess glycolipids, and chasing the Ag for 4, 12, 24, and 36 h at 37°C, using an iNKT cell hybridoma, N38-2C12, as a probe. Activation-induced IL-2 was determined and plotted as percentage of maximum, a value obtained at start of chase.
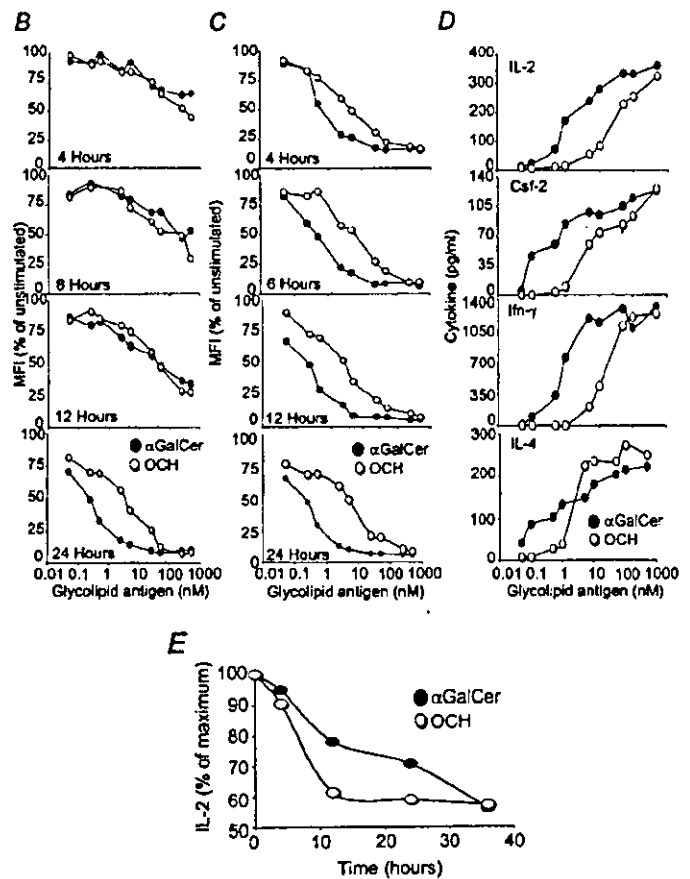
proliferation (Fig. 4*A*). In contrast, at a lower concentration (2.9 nM) of these same Ags, αGalCer induced a strong proliferative response; OCH induced a partial proliferative response, whereas 3,4D and NH elicited a very weak or no response, respectively (Fig. 4*A*). Furthermore, quantitation of the proliferative response revealed that αGalCer induced maximum proliferation at 5.75 nM, and OCH at 57.5 nM, whereas maximum expansion was not reached even with 575 nM of 3,4D (Fig. 4*B*). We also noted that stimulation with supraoptimal Ag concentrations does not result in increased proliferation, but actually reduces total iNKT cell expansion (Fig. 4*B*).

Together, the data reveal that, despite differences in K_{av} and the TCR β-chain repertoire, the altered lipid ligands induce proliferative response (Figs. 2, *B–F*, and 4, *A* and *B*). Therefore, the β-chain repertoire and the K_{av} of Ag-expanded iNKT cells were determined. TCR β-chain repertoire of iNKT cells following αGalCer, OCH, and 3,4D stimulation remains largely unaltered at

Ag concentrations inducing a maximum proliferative response, although a slight decrease in the percentage of Vb8-negative iNKT cells was noted (~35% of expanded iNKT (Fig. 4*C*) compared with ~45% for naive iNKT cells (Fig. 2*B*)). Additionally, very little if any difference was observed in the Vb repertoire of iNKT cells expanded with different suboptimal doses of αGalCer and OCH (data not shown). Interestingly, iNKT cell activation by 3,4D, but not αGalCer or OCH, resulted in the expansion of iNKT cells responding to Ag with higher K_{av} for αGalCer and OCH (Fig. 4*D* and Table II). Thus, high-avidity iNKT cells preferentially expand to suboptimal TCR engagement.

Cooperative glycolipid Ag recognition by iNKT cells

Self-Ag recognition must be finely tuned to prevent iNKT cell activation during physiological conditions, but respond rapidly to disturbances in cellular physiology. In other words, iNKT cells need to be very sensitive to modest changes in Ag concentration.

FIGURE 4. Activation of iNKT cells by suboptimal avidity Ag 3.4D in vitro causes selective expansion of high-avidity clones. *A*. C57BL/6 splenocytes were stimulated with the indicated concentrations of glycolipid Ags for 96 h. iNKT cell number and cell division history were determined using tetramers and CFSE (see *Materials and Methods*). *B*, Total iNKT cell number was determined following 96 h of Ag-stimulated culture. *C*, TCR β-chain repertoire of CD1d1-αGalCer- and -OCH-reactive cells following 96 h of in vitro iNKT cell stimulation with indicated concentrations of glycolipid Ags. *D*, C57BL/6 splenocytes were stimulated with the indicated glycolipid. The resulting iNKT cell population was reacted with the indicated concentration of CD1d1-αGalCer or CD1d1-OCH tetramers. From the binding isotherms, K_{av} was determined as described in Fig. 1. Binding reactions were performed at 4°C in the presence of sodium azide to prevent capping and internalization.
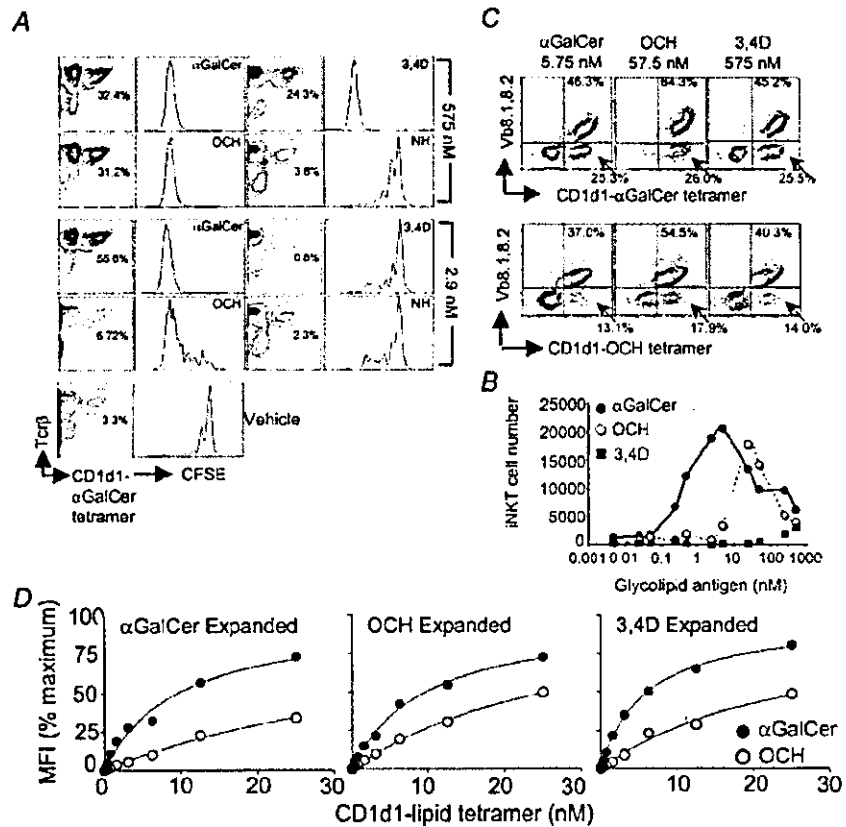
In biological systems, this kind of fine-tuning is often achieved by using cooperative ligand-receptor interactions (33, 63). To determine whether cooperativity participates in sensitive glycolipid Ag recognition. this mode of interaction was determined by calculating the Hill coefficient (see *Materials and Methods*). The Hill coefficient of the interaction between the tetrameric Ag and the iNKT cell receptor was >2 (Fig. 5A and Table I). In stark contrast, all MHC class I-restricted TCR had a calculated Hill coefficient of ~1 (Fig. 5B and Table I), indicating a lack of cooperativity. Peptide binding to each H2K[b] monomer of the tetrameric molecule is an independent event. Saturation binding of the tetramer to the TCR with increasing concentration of added peptide indicates occupancy of all four sites (Fig. 5B). Furthermore, an analysis of the stoichiometry of class I H chain, β_2-microglobulin. and peptide following ligand exchange by Edman sequence determination (64) revealed a 1:1:1 ratio of the three components (data not shown). Thus, a Hill coefficient of 1 is not due to incomplete loading of the class I tetramer.

OCH is a structurally different Ag, particularly in the hydrophobic component thought to interact with CD1d1. Also, OCH interaction with CD1d1 has distinct kinetic parameters compared with αGalCer (Figs. 2F and 3E). Thus, to exclude the possibility that the biochemical or structural properties of αGalCer loading onto CD1d1 account for the observed cooperative response, Hill coefficient was measured for the binding of CD1d1-OCH to the Va14Ja18 TCR. As expected, we found that the Hill coefficient for CD1d1-OCH and CD1d1-αGalCer for the same Va14Ja18 TCR are very similar (Fig. 5C and Table II). Thus, Hill coefficient measurement does not reflect the loading properties of glycolipid Ags, but rather, it is the property of the Ag receptors with which it interacts.

To independently demonstrate cooperative Ag engagement by iNKT cells with multimeric Ags other than soluble, biotinylated monomers of CD1d1 and H2K[b] prepared in-house, we determined the Hill coefficients with commercially obtained dimeric IgG1-CD1d1 and IgG1-H2K[b] fusion molecules loaded with αGalCer and H60 peptide, respectively, for iNKT cells and H60-specific SPH60 CTL clone. iNKT cells demonstrated cooperative engagement of both dimeric and tetrameric Ag by the Va14Ja18 TCR (Fig. 5D and Table I). As expected, neither dimeric nor tetrameric H2K[b] cooperatively engaged their cognate TCR (Fig. 5D and Table I). Thus, we conclude that, in contrast to conventional T lymphocytes, glycolipid Ag recognition by iNKT cells involves cooperativity.

iNKT cell receptor appears to have distinct structure and/or organization

A plausible model for cooperative tetrameric Ag engagement by Va14Ja18 TCR is receptor partitioning and oligomerization within lipid rafts (50). To test this model, Hill coefficients for Ag-receptor interactions were determined for two representative iNKT hybridomas (N38-2C12 and N37-1H5a). NKT cell-enriched thymocytes. and two CTL clones (SPH60 and BH60), following disruption of their lipid rafts. Lipid rafts were disrupted by cholesterol depletion with methyl-β-cyclodextrin (65) or alternatively by filipin-mediated intercalation of this membrane microdomain (66). Disruption of lipid rafts did not alter the Hill coefficient for any of the interactions tested (data not shown), suggesting that these membrane microdomains are not critical for cooperative Ag engagement by iNKT cell receptor.

To further examine the structural properties of iNKT cell Ag receptor, we used fluorescence resonance energy transfer (FRET)

FIGURE 5. Cooperative engagement of multimeric CD1d1 by the Val4Jal8 TCR. A constant concentration of multimer (CD1d1 tetramer (A and C); H2Kᵇ tetramer (B); CD1d1 and H2Kᵇ dimers and tetramers (D)) was loaded with the indicated concentrations of Ag (αGalCer or OCH (A and C); peptide (B)) and reacted with freshly isolated NKT cell-enriched thymocytes (A), NKT hybridomas (A and C), or CTL clones (B). Binding was monitored as described in Fig. 1. From the binding curve, Hill plots and Hill coefficients (h), represented beneath the Ag-binding curves, were derived (see Materials and Methods). Tetramers of CD1d1 and H2Kᵇ were generated by fluorochrome-conjugated streptavidin-mediated tetramerization of biotinylated monomers. Binding of dimers of CD1d1 and H2Kᵇ, owing to their fusion to IgG1 H chains, were detected with Alexa Flour 647- or PE-conjugated Fab specific for the Fc portion. The high regression coefficient (>0.90) for all Hill plots indicates that the calculated h values are significant. All binding reactions were performed at 4°C in the presence of sodium azide to prevent capping and internalization.
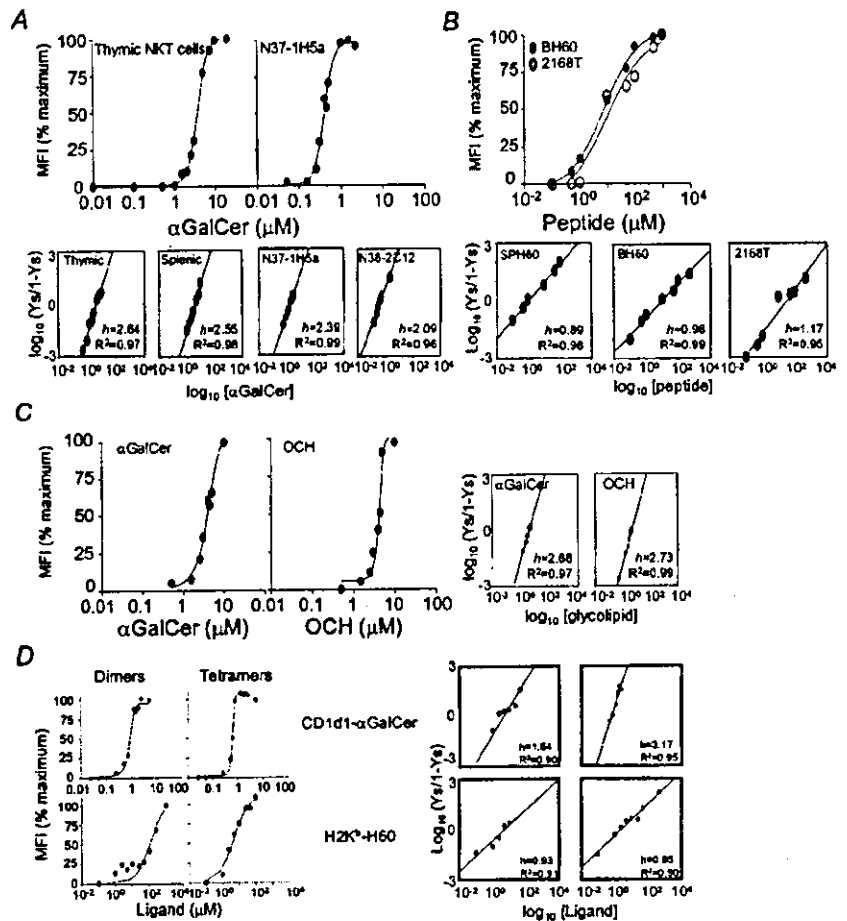
measurements between CD1d1 and H2Kᵇ multimers and Abs specific for components of the TCR complex. In the course of our studies, we observed that costaining of iNKT cells ex vivo by allophycocyanin- or PE-conjugated CD1d1 tetramers and PE- or allophycocyanin-TCRβ (clone H57-597) or anti-CD3ε (clone 145-2C11) Abs resulted in large and repeatable increase in FL3 channel fluorescence in a properly compensated flow-cytometric experiment (Fig. 6, A (iNKT cell hybridoma N38-2C12) and B (thymic iNKT cells)). Such large FRET shift was not observed with high-intensity staining Abs specific for cell surface molecules not within the TCR complex (e.g., anti-CD44, clone IM7; Fig. 6). As PE and allophycocyanin have overlapping fluorescence emission and absorption spectra, respectively, it was likely that this result was a consequence of nonradiative FRET. This hypothesis was tested by running samples on the flow cytometer with the red diode laser (emission, 635 nm) and its FL4 filter switched off. Indeed, we still observed FL3 fluorescence only when costaining with CD1d1 multimers and TCR complex-specific Abs. The large FRET observed upon tetramer-anti-TCRβ/anti-CD3ε binding to iNKT cells presented an opportunity to test the hypothesis that the structural orientation and/or organization of Val4Jal8 TCR are distinct from αβ TCR of conventional CTL. When H60-specific CTL were costained in a manner identical with that of iNKT cells, and analysis was restricted to equivalent MFI of anti-TCRβ or anti-CD3ε and H2Kᵇ multimer, very little FRET was detected (Fig. 6A). Similarly, we observed FRET using PE-conjugated CD1d1 tetramers and allophycocyanin-conjugated anti-TCRβ or anti-CD3ε Abs (data not shown). FRET between CD1d1-αGalCer tetramers and

TCRβ on iNKT cells directly correlated with the staining intensity, even at relatively low concentrations (~2.5 nM; Fig. 6C). In contrast, no FRET between H2Kᵇ tetramers and TCRβ or CD3ε was observed, even with saturating concentrations of H2Kᵇ tetramers (~250 nM; Fig. 6C). FRET is exquisitely sensitive to small changes in donor and acceptor fluorochrome distances (FRET, ~r⁶). Thus, these results strongly suggest that iNKT cell receptor has a distinct structure and/or organization, resulting in shorter distance between donor and acceptor fluorochromes used.

Discussion

In summary, our findings demonstrate that iNKT cell receptors recognize glycolipid Ags with avidities similar to, if not higher than, those of immunodominant, high-affinity αβ TCR of conventional T cells. In contrast to CTL, which recognize Ag over a large avidity range (20–220 nM), iNKT cells efficiently recognize Ag within a narrow window of avidity (10–40 nM). Interestingly, although the TCR-Ag dwell time for αGalCer and OCH are very similar, TCR down-regulation as well as the proliferative and cytokine response of iNKT cells to these Ags directly correlated with avidity for Ag. Strikingly, both αGalCer- and OCH-bound CD1d1 tetramers and dimers display cooperative engagement of the iNKT cell receptor, a property that CTL clones tested in this study lack. Additional data revealed FRET between specific combinations of fluorochromes conjugated to CD1d1 tetramers or dimers (data not shown) and TCR β-chain or CD3ε-specific Abs. These findings
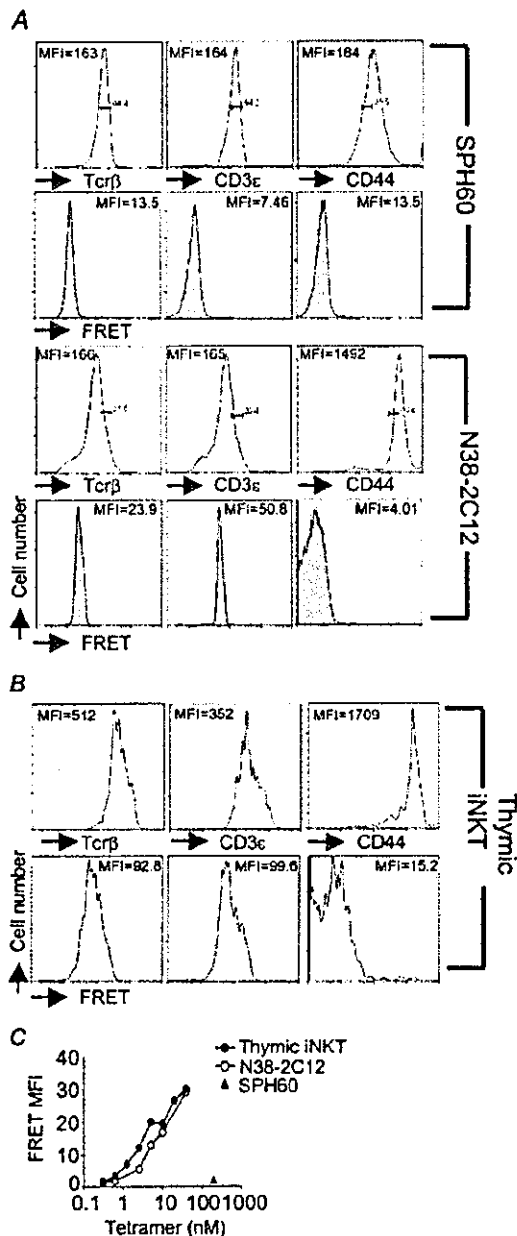
FIGURE 6. iNKT cell receptor has distinct structure and/or organization. CTL clone SPH60 (*A*), iNKT hybridoma N38-2C12 (*A*), and thymic iNKT cells (*B*) were reacted with allophycocyanin-conjugated H2K^b-H60 and CD1d1-αGalCer tetramers, respectively. They were also reacted with PE-conjugated Abs against TCRβ (H57-597; specific for TCRβ chain FG loop), CD3ε, or CD44. FRET was measured as the fluorescence in the FL3 channel, with the red diode laser off. CD1d1- and H2K^b-tetramer concentrations were adjusted to obtain equal MFI of tetramer staining. Considering that the 488-nm emission of the argon-ion laser cannot excite allophycocyanin, fluorescence detected in the FL3 channel is due to FRET-mediated allophycocyanin excitation. FRET-induced fluorescence intensity is indicated as a function of CD1d1-αGalCer tetramer concentration (*C*). All binding reactions were performed at 4°C in the presence of sodium azide to prevent capping and internalization.

suggest that the iNKT cell receptor structure and/or organization may be distinct from conventional αβ TCR.

Conventional T cells recognize peptide Ags with a wide range of avidities and dwell times (23–25, 28, 29). In contrast, strong

recognition of αGalCer and OCH, poor recognition of 3,4D, and no recognition of NH (19), by the Va14Ja18 TCR with distinct K_{av} points toward a narrow kinetic window for iNKT cell activation. We demonstrate that both optimal Ag concentration and relative avidity are essential to elicit a strong proliferative response by iNKT cells. Interestingly, as observed with conventional T cell effector functions (56), iNKT cells exhibit hierarchical functional consequences to Ag quality and concentration. In support of our previous study (19), we also find a dissociation from a clear avidity-concentration dependence in IL-4 secretion following OCH compared with αGalCer stimulation. Both low Ag concentration and low K_{av} are sufficient for selective IL-4 secretion and iNKT cell proliferation. In contrast, higher K_{av} and Ag concentration are required for IFN-γ response. Consistent with this conclusion is the finding that dendritic cells presenting a high concentration of the high K_{av} Ag αGalCer induce sustained IFN-γ response from iNKT cells (67). In this regard, iNKT cell response closely follows the principle of Ag concentration threshold set for IFN-γ and IL-4 responses elicited by conventional T cells (68).

Due to their potent immunoregulatory properties, therapeutic modulation of iNKT cell number and functional responses has been proposed for prevention of autoimmunity as well as for the enhancement of immune responses to tumors and vaccines. In the nonobese diabetic mouse model of autoimmune type I diabetes, iNKT number and function are low (43, 69, 70). Increasing the iNKT cell number (71–73) or the αGalCer treatment-induced Th2 bias (17, 18, 74) effectively reduces the incidence of type I diabetes in nonobese diabetic mice. Our data demonstrate that distinct glycolipid administration regimens may be required to induce tolerizing activity compared with IFN-γ-dependent antitumor and adjuvant properties of iNKT cells.

The natural self-Ag recognized by iNKT cells and its structural relationship to αGalCer remain unknown. However, we recently discovered that a cell line deficient in β-glucosylceramide (βGlcCer) is defective in the presentation of a self-Ag to iNKT cell hybridomas (15). Together with the evidence that the defect was not due to altered folding, intracellular traffic of CD1d1, or recognition of βGlcCer itself, these results suggest that βGlcCer is either a precursor or an essential factor in the synthesis and/or loading of a natural Ag. Thus, it is possible that the elusive self-Ag may be αGlcCer or a similar compound. Further support for the hypothesis that a self-Ag similar to αGalCer is recognized is the finding that transgenic overexpression of CD1d1 results in preferential deletion of Vb8.1,8.2$^+$ iNKT cells (75). This result is fully consistent with our finding that Vb8.1,8.2$^+$ iNKT cells have a higher K_{av} for αGalCer and OCH than Vb8.1,8.2-negative iNKT cells. Furthermore, the high K_{av} binding of CD1d1-αGalCer with Vb8.1,8.2$^+$ Va14Ja18 TCR is consistent with the high K_{av} binding of dimeric Ag to similar TCR (27). Importantly, for the first time, we demonstrate that the repertoire and Ag K_{av} of iNKT cell receptors are regulated during proliferation and result in selection of high-avidity iNKT cells under conditions of suboptimal stimulation. These data, taken together, suggest that the narrow kinetic window of recognition of αGalCer and its analogues is reflective of the parameters of natural self-Ag recognition.

The 2C transgenic TCR exhibits differing peptide Ag binding modes on naive and effector cells, suggesting cooperativity (50). The existence of two TCR αβ molecules within a single CD3 complex was evoked to explain this result (50). However, recent data suggest that the stoichiometry of TCR αβ assembly with CD3 complex is 1:1 (76). Whether this stoichiometry changes during CTL activation remains to be established. Using tetramers of CD1d1 and H2K^b, we demonstrate cooperative Ag engagement of glycolipid Ags by iNKT cell receptors but not that of peptidic Ags